Supporting Information

Peroxide-Driven Hydroxylation of Small Alkanes Catalyzed by an Artificial P450BM3 Peroxygenase System

Jie Chen,[†,‡] Fanhui Kong,[†] Nana Ma,[†,‡] Panxia Zhao,[†,‡] Chuanfei Liu,[†] Xiling Wang,[†] and Zhiqi Cong[†,‡,*]

[†]CAS Key Laboratory of Biofuels and Shandong Provincial Key Laboratory of Synthetic Biology, Qingdao Institute of Bioenergy and Bioprocess Technology, Chinese Academy of Sciences, Qingdao, Shandong, 266101, China

[‡]University of Chinese Academy of Sciences, Beijing, 100049, China

* To whom correspondence should be addressed. E-mail: congzq@qibebt.ac.cn

Experimental Section

Materials

All chemical reagents were purchased from commercial sources (e.g. Aldrich, TCI, and Alladin) and used without further purification until otherwise noticed. Propane and butane were purchased from Qingdao Dehai weiye technology co. LTD.

Expression and Purification of P450BM3

The heme domain of Cytochrome P450BM3 and its variants were respectively cultured and purified according to reported methods.[1] All of purified proteins were characterized by SDS pages (Figures S1-S6).

The formation of a ferrous CO complex was confirmed by UV-visible spectral change through the reduction of ferric heme of the wild type P450 and its mutants by addition of $Na_2S_2O_4$ in the presence of carbon monoxide (CO) (Figure S7).[2]

The concentrations of P450BM3 and its variants were measured by Hemochrome binding assay.[3] A pyridine solution was made by combining pyridine (1.75 mL) and 1 M aqueous of NaOH (0.75 mL). The solution was mixed at room temperature then centrifuged for 30 s at 5000 rpm to remove excess aqueous base. To a cuvette containing 0.75 mL of protein solution in phosphate buffer (0.1 M, pH 8.0), 0.25 mL of the pyridine solution was added followed by 2 mg of sodium dithionite. A UV-vis spectrum was recorded immediately. Hemoprotein concentration was determined from the absorbance of the hemochrome complex using extinction coefficients of ε_{418} = 196 mM^{-1} cm^{-1}. Absorbance was assigned as the difference between the peak max at 418 nm and the baseline at 420 nm as determined by extrapolating from two points on either side of the hemochrome peak (390 nm and 450 nm).

Mutagenesis

All the mutations were made by PCR based site-directed mutagenesis and verified by DNA sequencing. The F87 mutations were made as described.[1]

The F87A/T268 mutations was in F87A background. The primers used were as follows:

primer	sequence
T268A-F	5’- GCGACAAGTGGTCTTTTATCATTTGC -3’
T268V-F	5’- GTGACAAGTGGTCTTTTATCATTTGC -3’
T268I-F	5’- ATCACAAGTGGTCTTTTATCATTTGC -3’
T268L-F	5’- CTGACAAGTGGTCTTTTATCATTTGC -3’
T268F-F	5’- TTCACAAGTGGTCTTTTATCATTTGC -3’
T268W-F	5’- TGGACAAGTGGTCTTTTATCATTTGC -3’
T268-R	5’- TTCGTGTCCCGCAATTAAGAATG -3’

The F87/T268I mutations were in F87A/T268I background. The primers used were as follows:

primer	sequence
F87A-F	5'- GCGACAAGCTGGACGCATGAAAAAAATTG -3'
F87G-F	5'- GGTACAAGCTGGACGCATGAAAAAAATTGGAA -3'
F87V-F	5'- GTGACAAGCTGGACGCATGA AAAAAATTGGAA -3'
F87I-F	5'- ATTACAAGCTGGACGCATGAAAAAAATTGAAAAAAGC -3'
F87L-F	5'- CTGACAAGCTGGACGCATGAAAAAAATTGGAA -3'
F87-R	5'- TAACCCGTCTCCTGCAAAATCACGTACAA -3'

The F87A/T268I/A82 mutations were in F87A/T268I background. The primers used were as follows:

primer	sequence
A82-F	5'- GTTAGCGACAAGCTGGACGCATG -3'
A82G-R	5'- CCGTCTCCACCAAAATCACGTACAAATTTAAG -3'
A82V-R	5'- CCGTCTCCCACAAAATCACGTACAAATTTAAG -3'
A82I-R	5'- CCGTCTCCAATAAAATCACGTACAAATTTAAG -3'
A82L-R	5'- CCGTCTCCCAGAAAATCACGTACAAATTTAAG -3'
A82F-R	5'- CCGTCTCCAAAAAAATCACGTACAAATTTAAG -3'
A82M-R	5'- CCGTCTCCCATAAAATCACGTACAAATTTAAG -3'
A82S-R	5'- CCGTCTCCGCTAAAATCACGTACAAATTTAAG -3'
A82T-R	5'- CCGTCTCCGGTAAAATCACGTACAAATTTAAG -3'
A82E-R	5'- CCGTCTCCTTCAAAATCACGTACAAATTTAAG -3'
A82C-R	5'- CCGTCTCCGCAAAAATCACGTACAAATTTAAG -3'
A82D-R	5'- CCGTCTCCATCAAAATCACGTACAAATTTAAG -3'
A82N-R	5'- CCGTCTCCATTAAAATCACGTACAAATTTAAG -3'

The F87A/T268I/A184 mutations were in F87A/T268I background. The primers used were as follows:

mutation	sequence
A184V-F	5'- CACTGGATGAAGTGATGAACAAGCTG -3'
A184I-F	5'- CACTGGATGAAATCATGAACAAGCTG -3'
A184L-F	5'- CACTGGATGAACTGATGAACAAGCTG -3'
A184M-F	5'- CACTGGATGAAATGATGAACAAGCTG -3'
A184F-F	5'- CACTGGATGAATTTATGAACAAGCTG -3'
A184T-F	5'- CACTGGATGAAACCATGAACAAGCTG -3'
A184Q-F	5'- CACTGGATGAACAGATGAACAAGCTG -3'
A184N-F	5'- CACTGGATGAAAATATGAACAAGCTG -3'
A184-R	5'- CACGGACCATACTTGTAATAAATGGATGAG -3'

Recombination of P450 BM-3 Variants.

Beneficial mutations selected from the triple mutations F87A/T268I/A82 (T, S, V, M), F87A/T268I/A184 (V, I, L) were recombined. The F87A/T268I/A82/A184 mutations were also made by PCR to introduce A82 into the triple mutations F87A/T268I/A184. The primers used were as above.

General procedure for hydroxylation of propane and *n*-butane

P450BM3 (0.5 μM) was transferred to a glass sample bottle containing propane or *n*-butane-saturated phosphate buffer (0.1 M, pH 8.0) and *N*-(ω-imidazol-1-yl hexanoyl)-*L*-phenylalanine (Im-C6-Phe) (500 μM, dissolved in pH 8.0 phosphate buffer). The reaction was initiated by the addition of H_2O_2 (20 mM, dissolved in pH 8.0 phosphate buffer). Then the reactor was immediately equipped with an alkane balloon and the air in the bottle was replaced by the alkane gas for 2 min. The reaction mixture was incubated in water bath at 25℃ for 30 min. After the reaction, the mixture was quenched and extracted with 1 mL of methyl tertiary butyl ether (for propane reactions) or ethyl acetate (for *n*-butane reactions), and the organic phase was separated and dried with sodium sulphate anhydrous. The product was analyzed by gas chromatography (GC) by 3-pentanol (for propane reactions) or 2-hexanol (for *n*-butane reactions) as an internal standard. The product distribution was also determined by GC (for the typical analytic results see Figures S8-S9). Control reactions performed by repeating these steps in the absence of Im-C6-Phe.

General procedure for hydroxylation of *n*-pentane and *n*-hexane

P450BM3 (0.5 μM) was transferred to a glass sample bottle containing 0.1 M, pH 8.0 phosphate buffer, alkane (4 mM, dissolved in methanol (10% vol/vol)) and Im-C6-Phe (500 μM, dissolved in pH 8.0 phosphate buffer). The reaction was initiated by the addition of H_2O_2 (20 mM, dissolved in pH 8.0 phosphate buffer). The reaction mixture was incubated in water bath at 25℃ (in the case of *n*-pentane reactions at 4℃) for 30 min. After the reaction, the mixture was quenched and extracted with 1 mL of ethyl acetate, and the organic phase was separated and dried with sodium sulphate anhydrous. The product was analyzed by gas chromatography (GC) by 3-pentanol (for *n*-hexane reactions) or 2-hexanol (for *n*-pentane reactions) as an internal standard. The product distribution was also determined by GC (for the typical analytic results see Figures S10-S11). Control reactions performed by repeating these steps in the absence of Im-C6-Phe.

Gas Chromatography

After the reaction, the reaction mixture was extracted with 1 mL of ethyl acetate (or methyl tertiary butyl ether), and the organic phase was separated and dried with sodium sulphate anhydrous. The product analysis was performed on a Shimadzu GC-2010 plus gas chromatograph equipped with a HP-INNOWAX column (length: 30 m, internal diameter: 0.25 mm, film thickness: 0.5 μm, Agilent, USA), a flame ionization detector, and an AOC-20i auto sampler system. The analytical conditions were as follows:

For propane reactions: splitting ratio: 1/9, temperature program: injector 260 ºC, detector 260 ºC, 40 ºC oven for 1min, then 5 ºC/min gradient to 55 ºC for 2min, 10ºC /min gradient to 80 ºC, 40ºC /min gradient to 120 ºC, 60 ºC/min gradient to 240 ºC and then 240 ºC for 3 min (total 14.50 min).

For butane reactions: splitting ratio: 1/9, temperature program: injector 260 ºC, detector 260 ºC, 60 ºC oven for 1min, then 10 ºC/min gradient to 100 ºC, 5 ºC /min gradient to 120 ºC, 60 ºC/min gradient to 240 ºC and then 240 ºC for 3 min (total 14.00 min).

For pentane reactions: splitting ratio: 1/9, temperature program: injector 260 ºC, detector 260 ºC, 80 ºC oven, then 10 ºC/min gradient to 100 ºC, 5 ºC/min gradient to 130 ºC, 10 ºC/min gradient to160 ºC, 60 ºC/min gradient to 240 ºC and then 240 ºC for 2 min (total 14.33 min).

For hexane reactions: splitting ratio: 1/9, temperature program: injector 260 ºC, detector 260 ºC, 80 ºC oven, then 10 ºC/min gradient to 160 ºC, 60 ºC/min gradient to 240 ºC and then 240 ºC for 2 min (total 11.33 min).

Chiral separation

For the chiral separation, all the alkane reaction mixtures were extracted with 1 mL methyl tertiary butyl ether, and the organic phase was separated and dried with sodium sulphate anhydrous. The chiral analysis was performed on a Shimadzu GC-2010 plus gas chromatograph equipped with a CP-Chirasil Dex CB column (length: 25 m, internal diameter: 0.25 mm, film thickness: 0.25 µm, Agilent, USA), a flame ionization detector, and an AOC-20i auto sampler system. The products were identified relative to authentic standards by their retention time. The analytical conditions were as follows:

For 2-butanol: splitting ratio: 1/9, temperature program: injector 250 ºC, detector 250 ºC, 40 ºC oven for 3min, then 1 ºC/min gradient to 45ºC for 5 min, 10 ºC /min gradient to 60 ºC for 1 min, 30 ºC/min gradient to 180 ºC for 2 min (total 21.50 min).

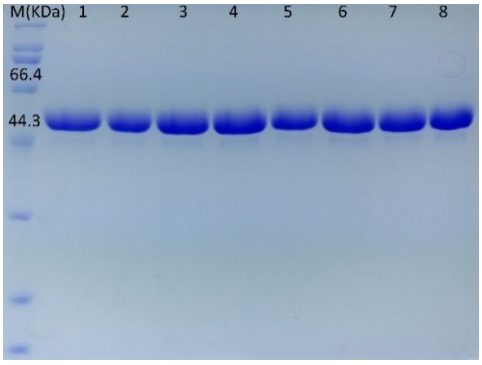

Figure S1 SDS Page of P450BM3 mutants. Lane1-8: F87A/T268A, F87A/T268V, F87A/T268I F87A/T268L, F87A/T268F, F87A/T268W, F87G/T268V, F87V/T268V.

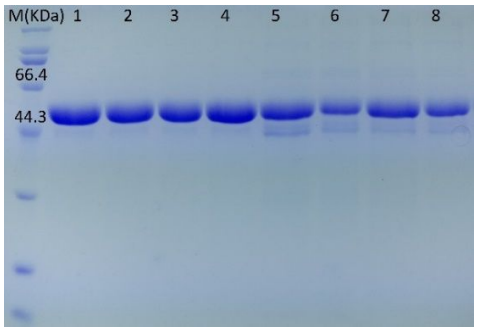

Figure S2 SDS Page of P450BM3 mutants. Lane1-8: F87G/T268I, F87V/T268I, F87I/T268I, F87L/T268I, F87A/T268I/A82V, F87A/T268I/A82I, F87A/T268I/A82L, F87A/T268I/A82G.

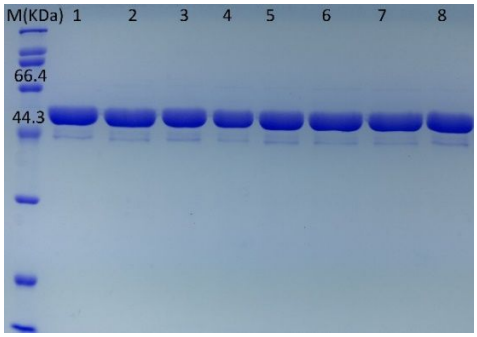

Figure S3 SDS Page of P450BM3 mutants. Lane1-8: F87A/T268I/A82F, F87A/T268I/A82E, F87A/T268I/A82C, F87A/T268I/A82D, F87A/T268I/A82T, F87A/T268I/A82S, F87A/T268I/A82N, F87A/T268I/A82M.

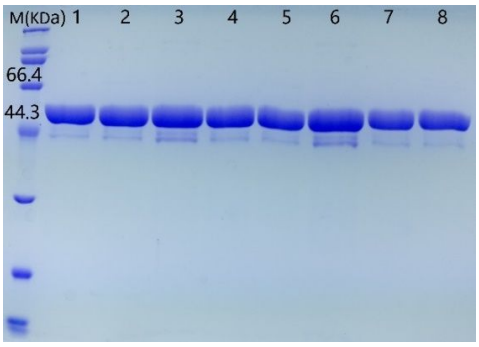

Figure S4 SDS Page of P450BM3 mutants. Lane1-8: F87A/T268I/A184V, F87A/T268I/A184I, F87A/T268I/A184L, F87A/T268I/A184M, F87A/T268I/A184F, F87A/T268I/A184T, F87A/T268I/A184Q, F87A/T268I/A184N.

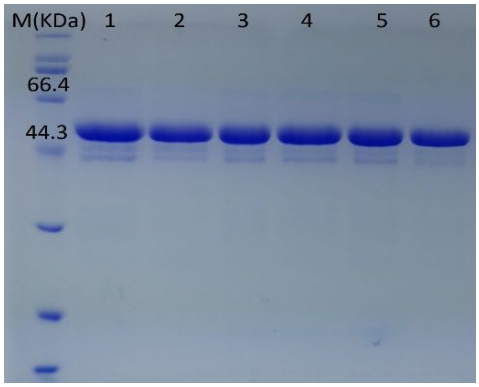

Figure S5 SDS Page of P450BM3 mutants. Lane1-8: F87A/T268I/A82S/A184V, F87A/T268I/A82S/A184I, F87A/T268I/A82S/A184L, F87A/T268I/A82M/A184V, F87A/T268I/A82M/A184I, F87A/T268I/A82M/A184L。

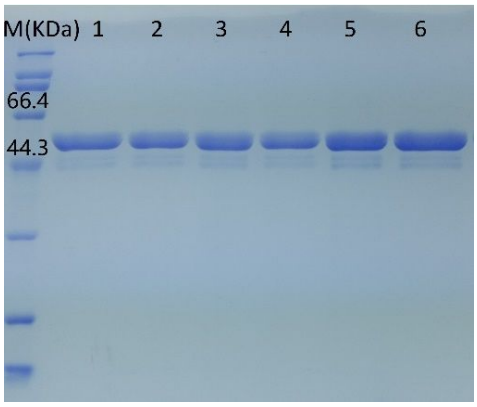

Figure S6 SDS Page of P450BM3 mutants. Lane1-8: F87A/T268I/A82V/A184V, F87A/T268I/A82V/A184I, F87A/T268I/A82V/A184L, F87A/T268I/A82T/A184V,

F87A/T268I/A82T/A184I, F87A/T268I/A82T/A184L。

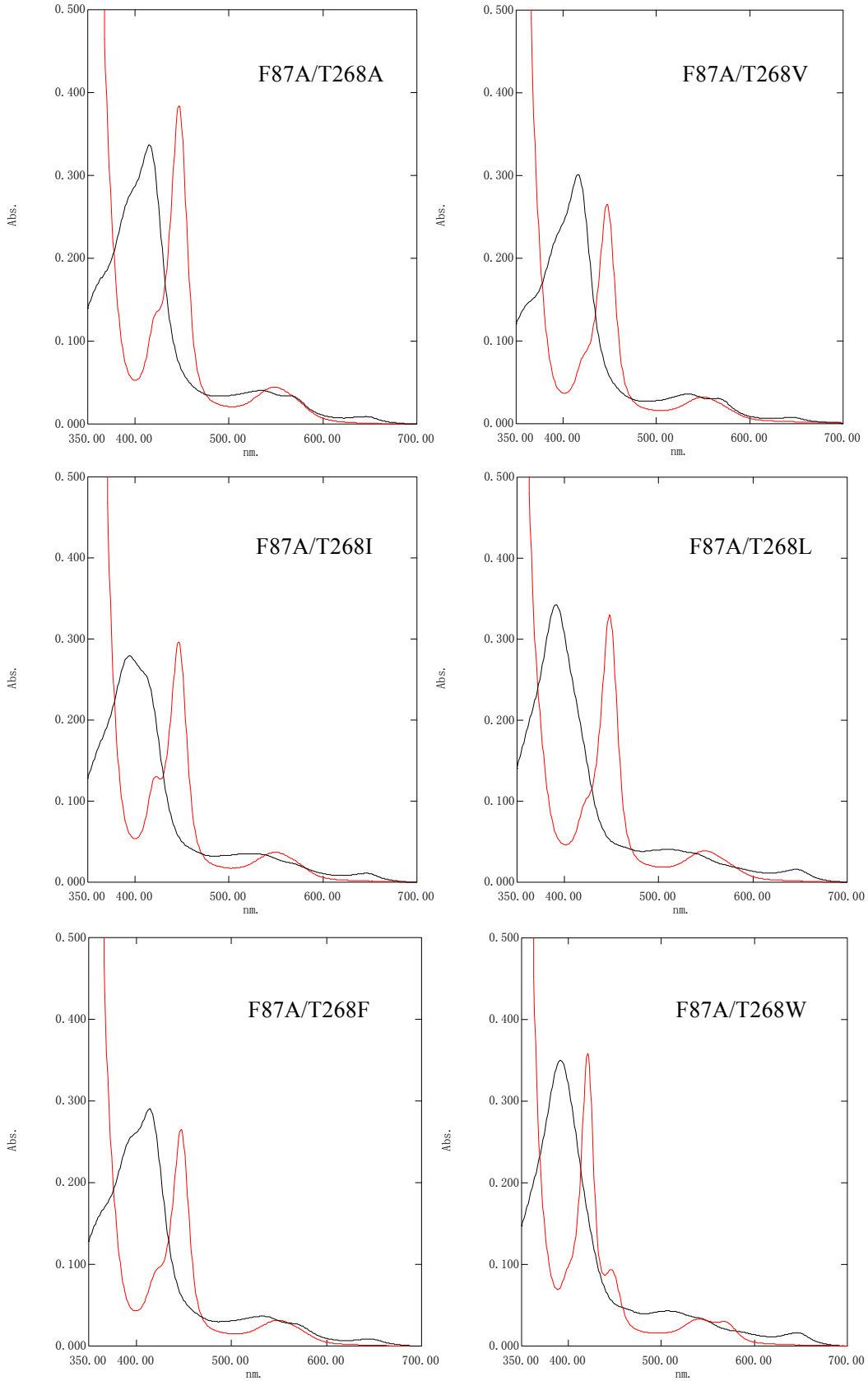

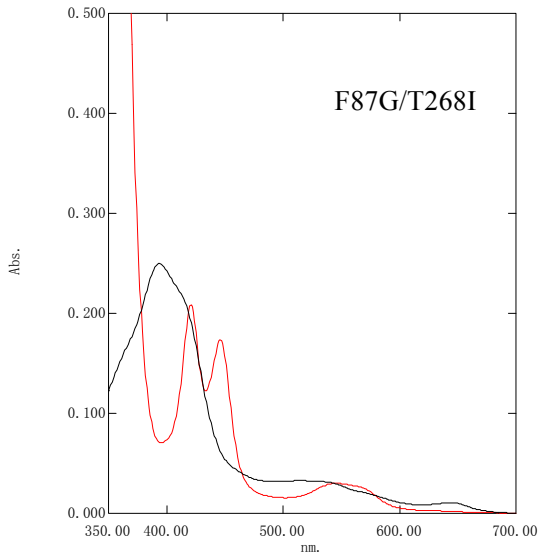
F87G/T268I
Abs.
0.500
0.400
0.300
0.200
0.100
0.000
350.00
400.00
500.00
600.00
700.00
nm.

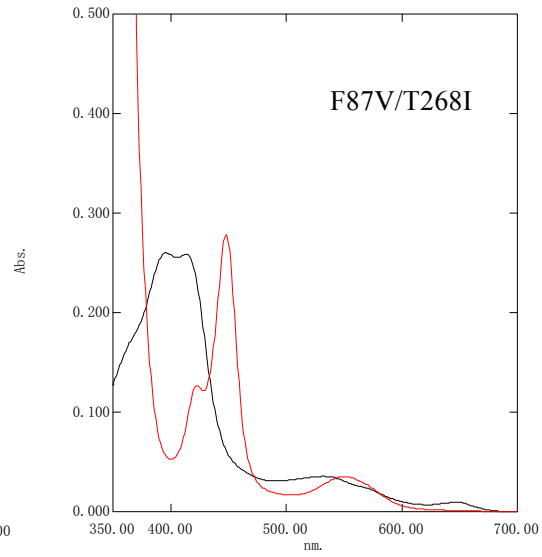
F87V/T268I
Abs.
0.500
0.400
0.300
0.200
0.100
0.000
350.00
400.00
500.00
600.00
700.00
nm.

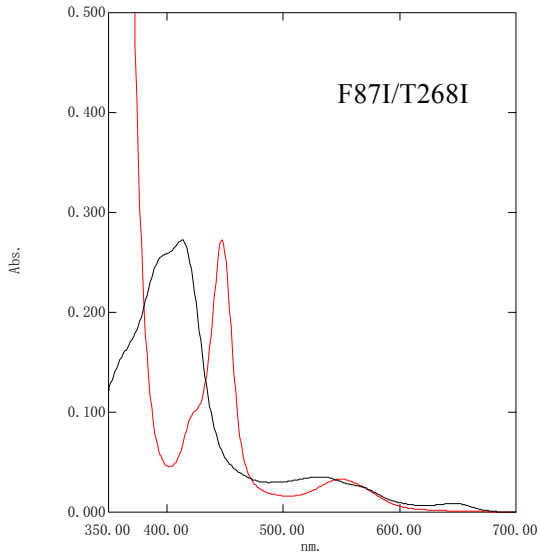
F87I/T268I
Abs.
0.500
0.400
0.300
0.200
0.100
0.000
350.00
400.00
500.00
600.00
700.00
nm.

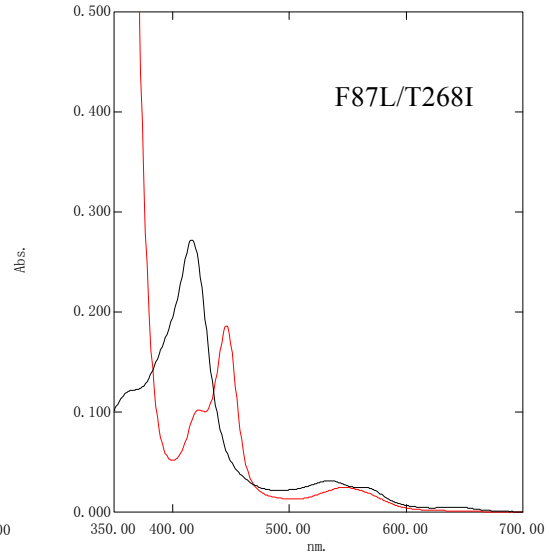
F87L/T268I
Abs.
0.500
0.400
0.300
0.200
0.100
0.000
350.00
400.00
500.00
600.00
700.00
nm.

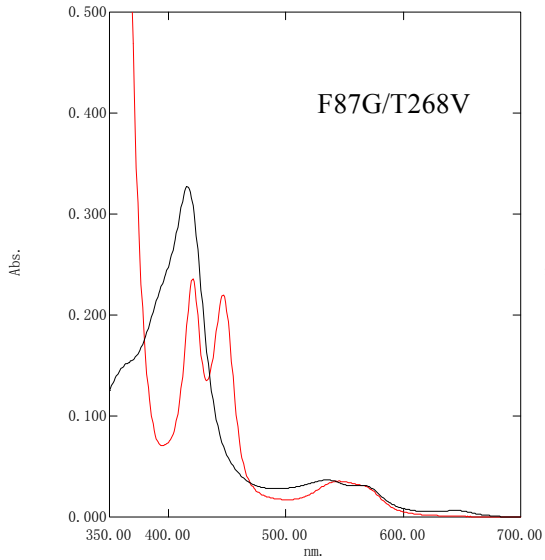
F87G/T268V
Abs.
0.500
0.400
0.300
0.200
0.100
0.000
350.00
400.00
500.00
600.00
700.00
nm.

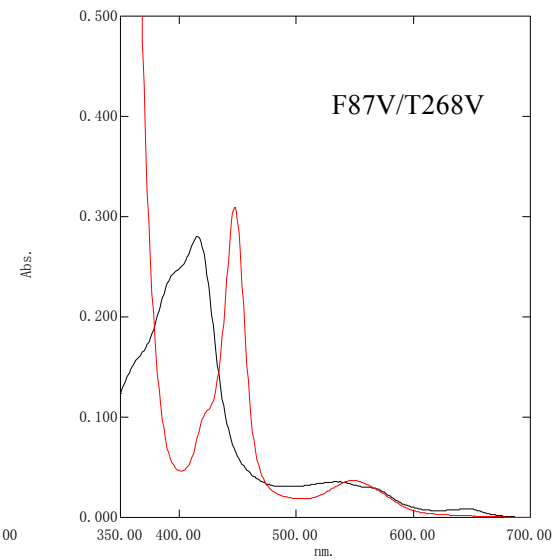
F87V/T268V
Abs.
0.500
0.400
0.300
0.200
0.100
0.000
350.00
400.00
500.00
600.00
700.00
nm.

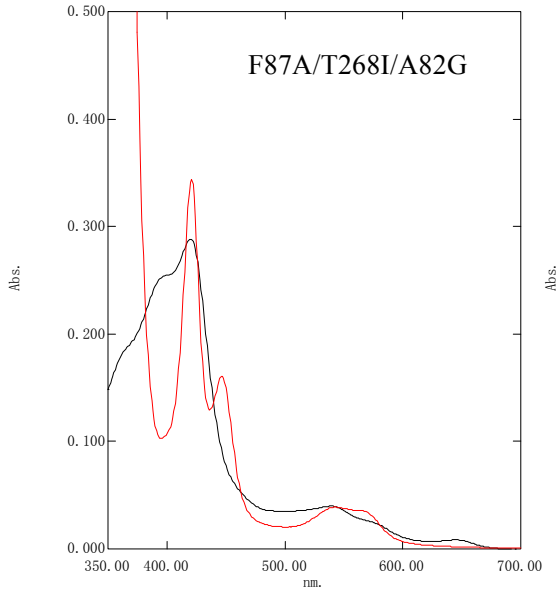
F87A/T268I/A82G
Abs.
0.500
0.400
0.300
0.200
0.100
0.000
350.00
400.00
500.00
600.00
700.00
nm.

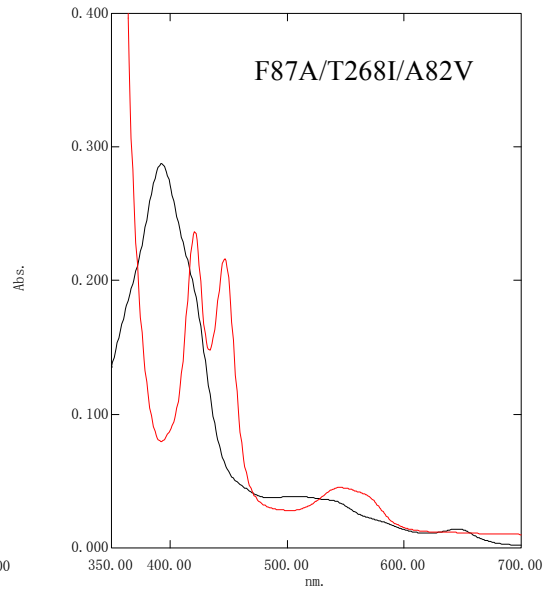
F87A/T268I/A82V
Abs.
0.400
0.300
0.200
0.100
0.000
350.00
400.00
500.00
600.00
700.00
nm.

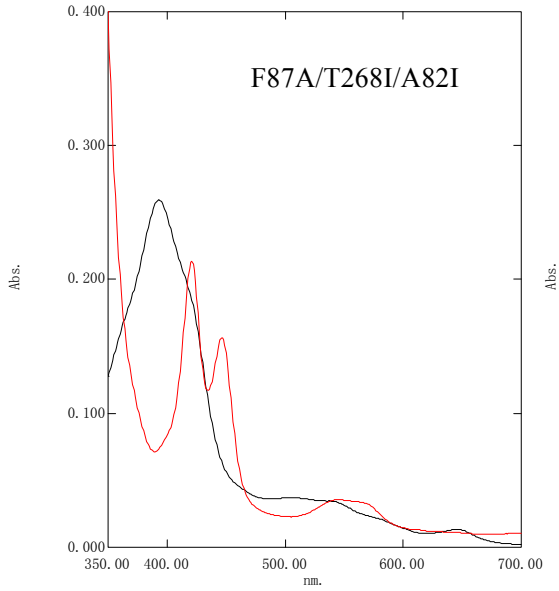
F87A/T268I/A82I
Abs.
0.400
0.300
0.200
0.100
0.000
350.00
400.00
500.00
600.00
700.00
nm.

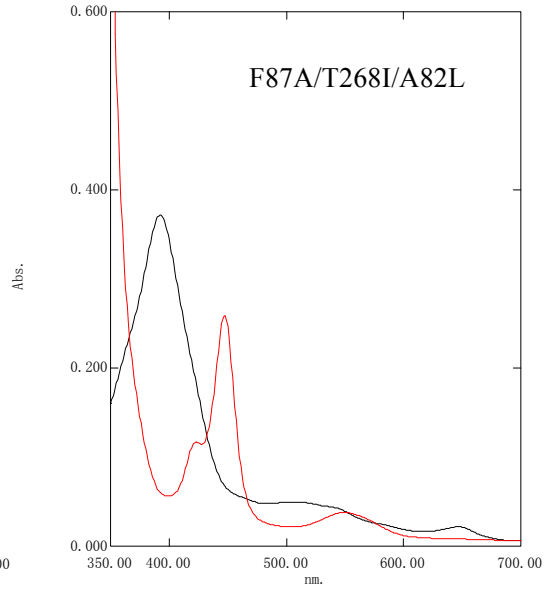
F87A/T268I/A82L
Abs.
0.600
0.400
0.200
0.000
350.00
400.00
500.00
600.00
700.00
nm.

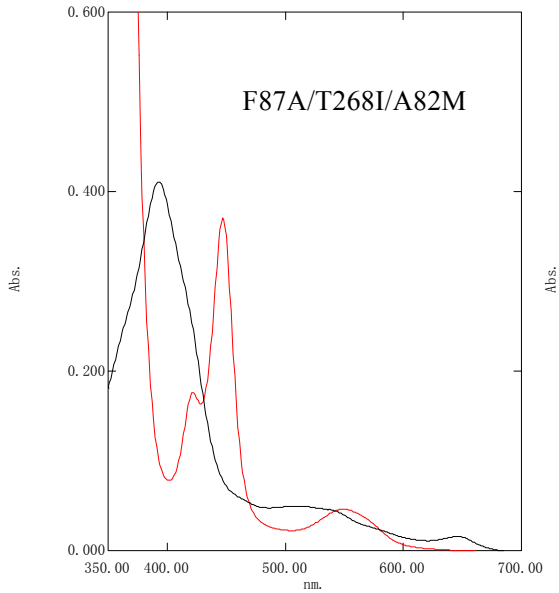
F87A/T268I/A82M
Abs.
0.600
0.400
0.200
0.000
350.00
400.00
500.00
600.00
700.00
nm.

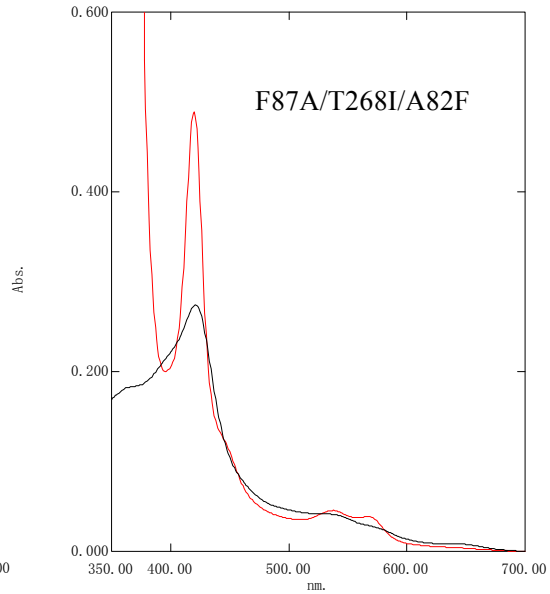
F87A/T268I/A82F
Abs.
0.600
0.400
0.200
0.000
350.00
400.00
500.00
600.00
700.00
nm.

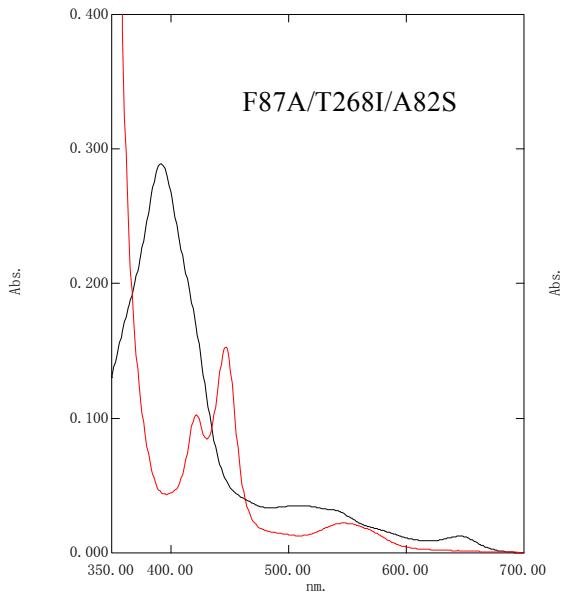
F87A/T268I/A82S
Abs.
0.400
0.300
0.200
0.100
0.000
350.00
400.00
500.00
600.00
700.00
nm.

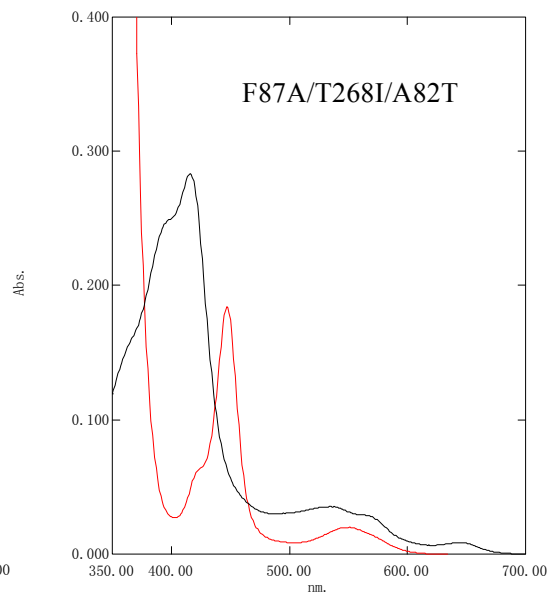
F87A/T268I/A82T
Abs.
0.400
0.300
0.200
0.100
0.000
350.00
400.00
500.00
600.00
700.00
nm.

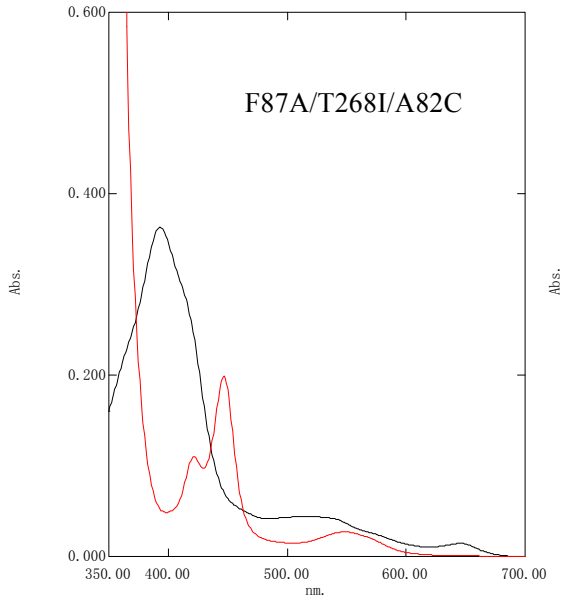
F87A/T268I/A82C
Abs.
0.600
0.400
0.200
0.000
350.00
400.00
500.00
600.00
700.00
nm.

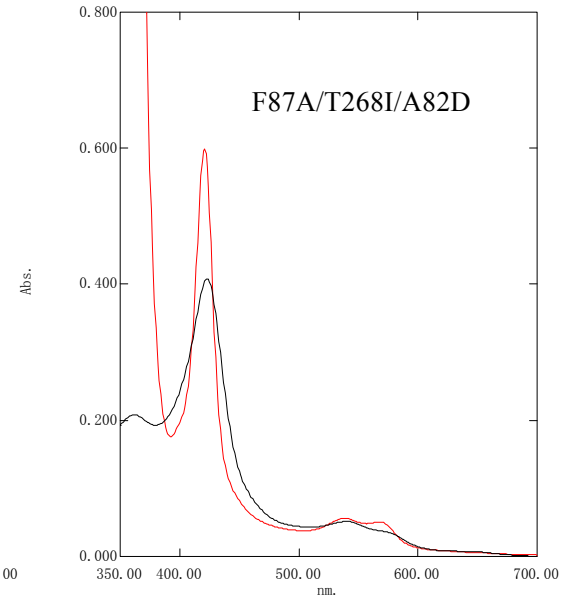
F87A/T268I/A82D
Abs.
0.800
0.600
0.400
0.200
0.000
350.00
400.00
500.00
600.00
700.00
nm.

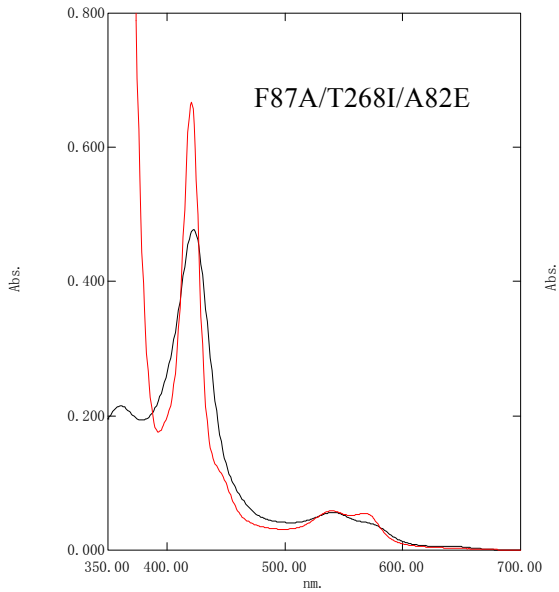
F87A/T268I/A82E
Abs.
0.800
0.600
0.400
0.200
0.000
350.00
400.00
500.00
600.00
700.00
nm.

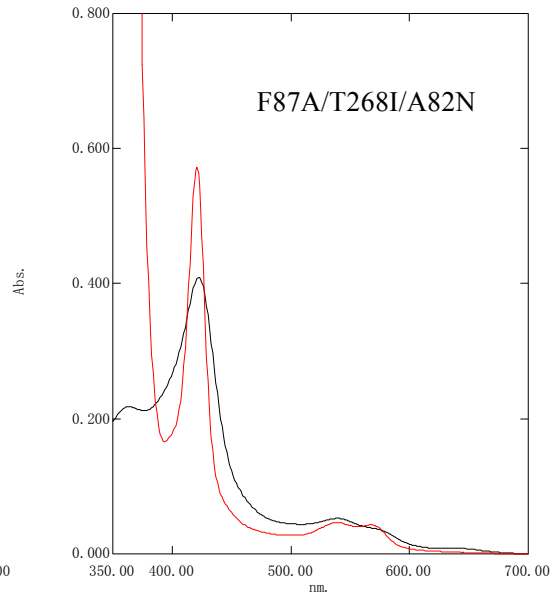
F87A/T268I/A82N
Abs.
0.800
0.600
0.400
0.200
0.000
350.00
400.00
500.00
600.00
700.00
nm.

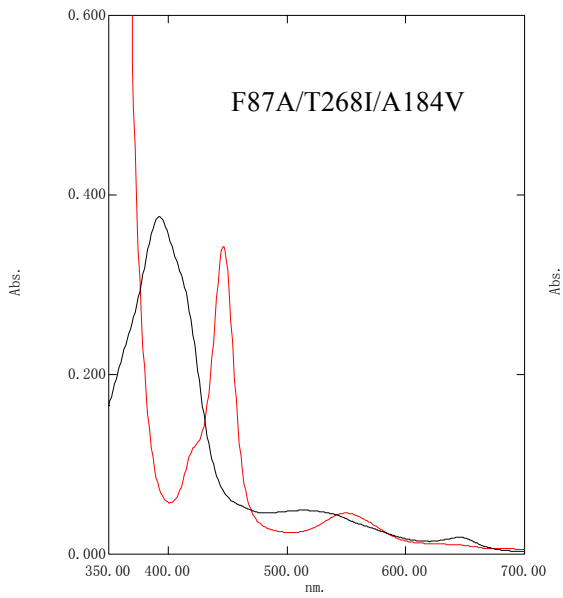
F87A/T268I/A184V
Abs.
0.600
0.400
0.200
0.000
350.00
400.00
500.00
600.00
700.00
nm.

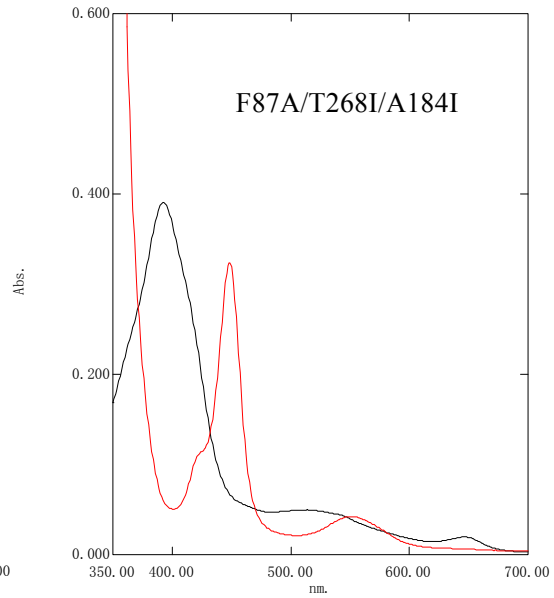
F87A/T268I/A184I
Abs.
0.600
0.400
0.200
0.000
350.00
400.00
500.00
600.00
700.00
nm.

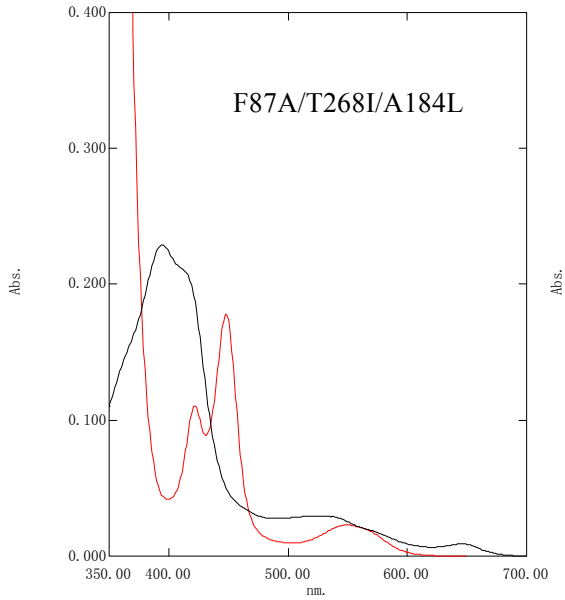
F87A/T268I/A184L
Abs.
0.400
0.300
0.200
0.100
0.000
350.00
400.00
500.00
600.00
700.00
nm.

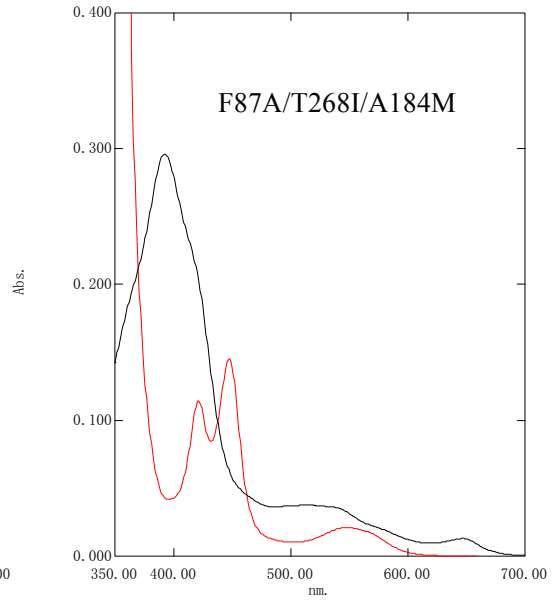
F87A/T268I/A184M
Abs.
0.400
0.300
0.200
0.100
0.000
350.00
400.00
500.00
600.00
700.00
nm.

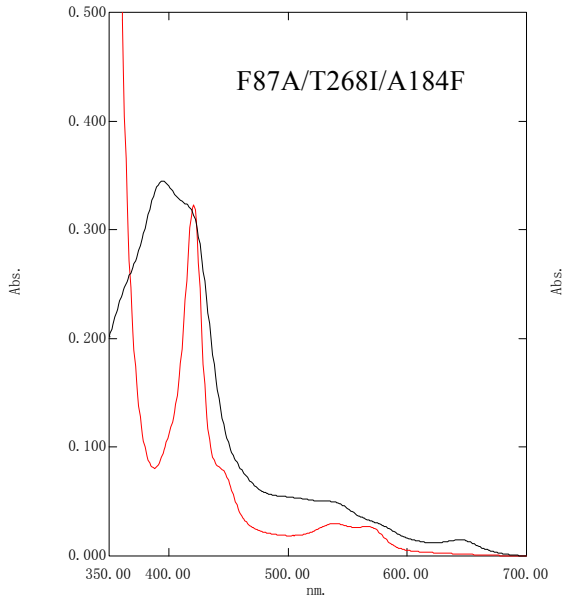
F87A/T268I/A184F
Abs.
0.500
0.400
0.300
0.200
0.100
0.000
350.00
400.00
500.00
600.00
700.00
nm.

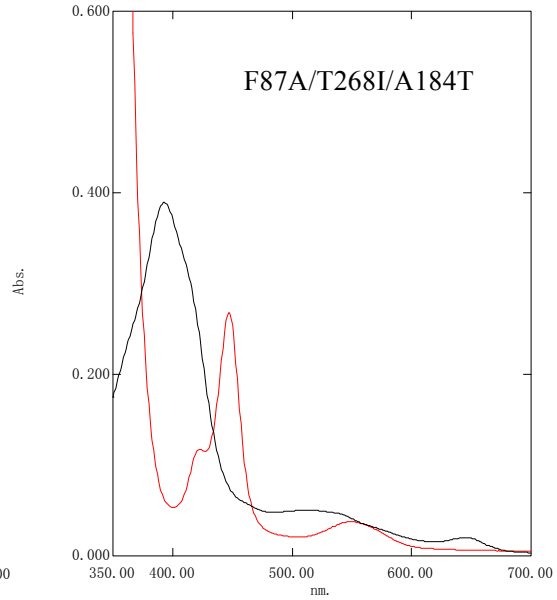
F87A/T268I/A184T
Abs.
0.600
0.400
0.200
0.000
350.00
400.00
500.00
600.00
700.00
nm.

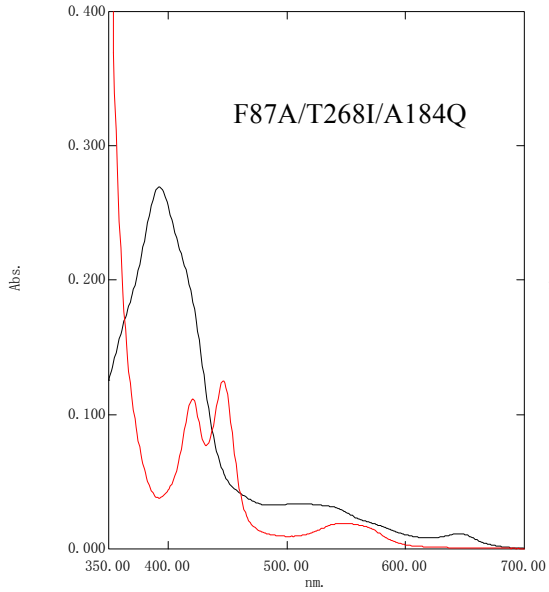
F87A/T268I/A184Q
Abs.
0.400
0.300
0.200
0.100
0.000
350.00
400.00
500.00
600.00
700.00
nm.

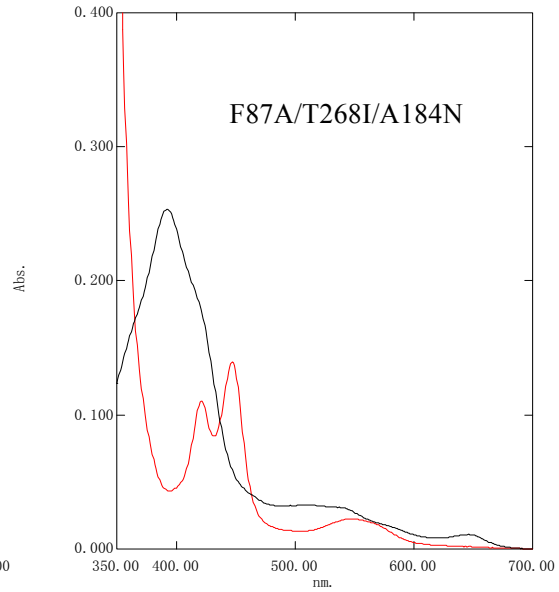
F87A/T268I/A184N
Abs.
0.400
0.300
0.200
0.100
0.000
350.00
400.00
500.00
600.00
700.00
nm.

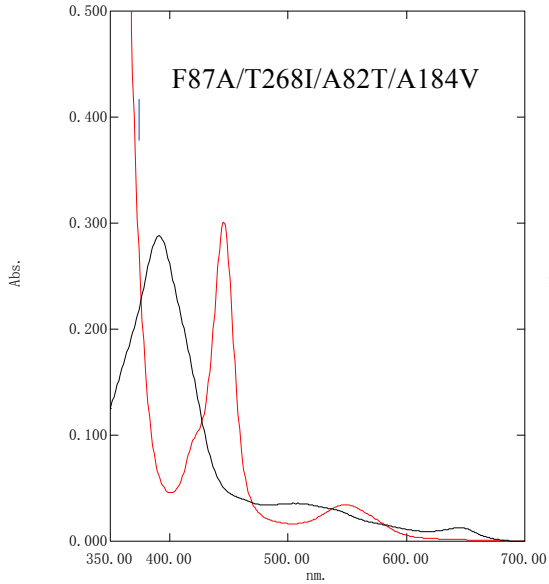
F87A/T268I/A82T/A184V
Abs.
0.500
0.400
0.300
0.200
0.100
0.000
350.00
400.00
500.00
600.00
700.00
nm.

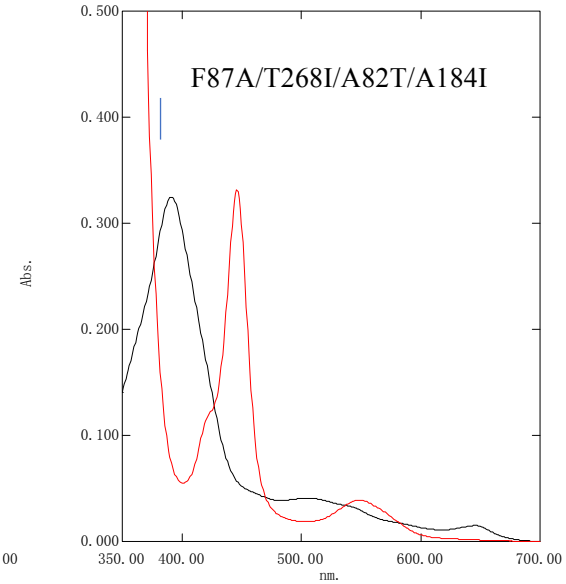
F87A/T268I/A82T/A184I
Abs.
0.500
0.400
0.300
0.200
0.100
0.000
350.00
400.00
500.00
600.00
700.00
nm.

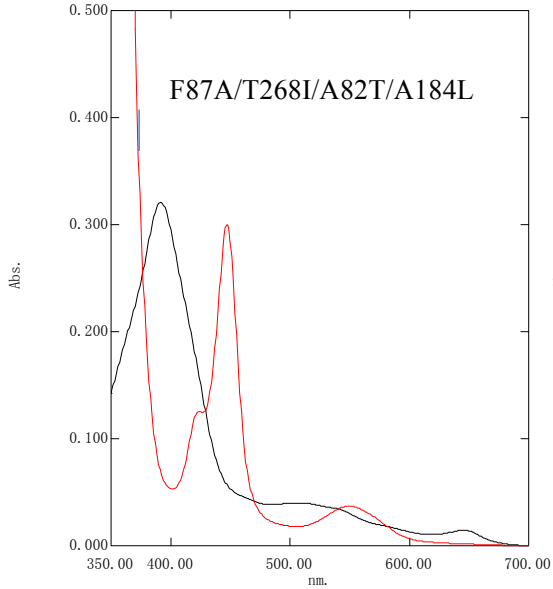
F87A/T268I/A82T/A184L
Abs.
0.500
0.400
0.300
0.200
0.100
0.000
350.00
400.00
500.00
600.00
700.00
nm.

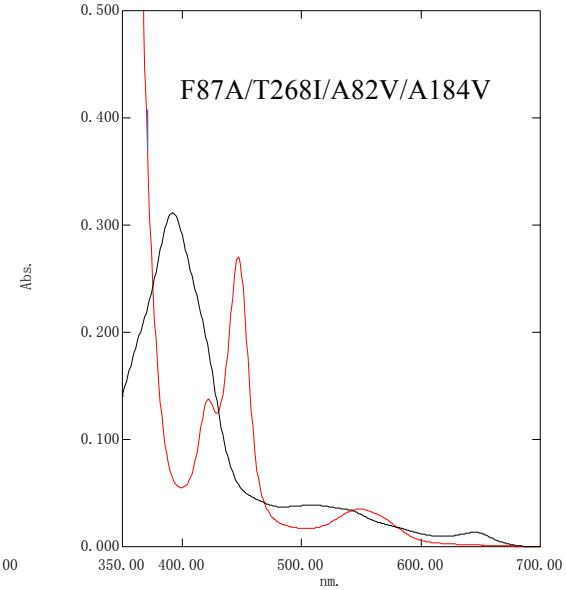
F87A/T268I/A82V/A184V
Abs.
0.500
0.400
0.300
0.200
0.100
0.000
350.00
400.00
500.00
600.00
700.00
nm.

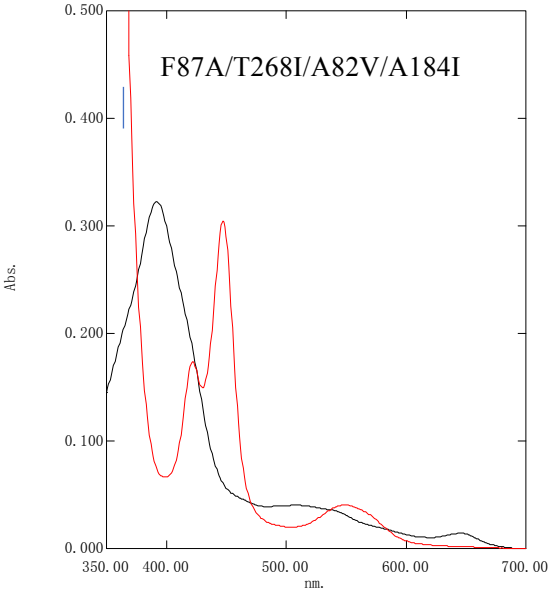
F87A/T268I/A82V/A184I
Abs.
0.500
0.400
0.300
0.200
0.100
0.000
350.00
400.00
500.00
600.00
700.00
nm.

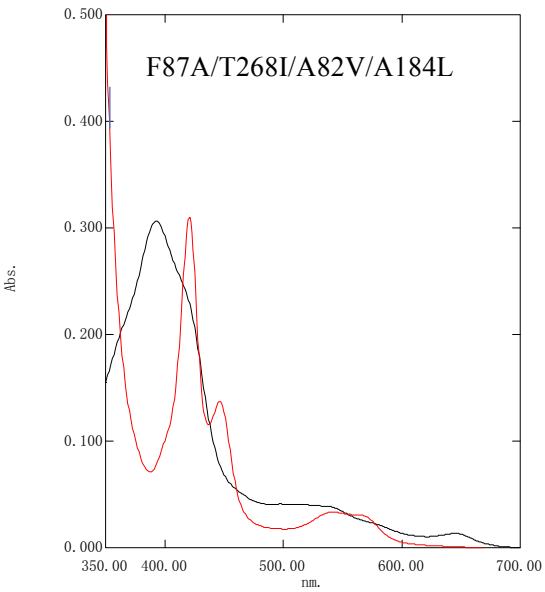
F87A/T268I/A82V/A184L
Abs.
0.500
0.400
0.300
0.200
0.100
0.000
350.00
400.00
500.00
600.00
700.00
nm.

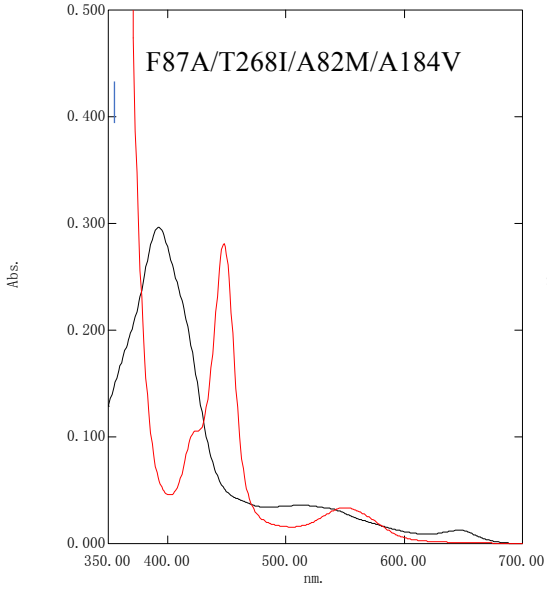
F87A/T268I/A82M/A184V
Abs.
0.500
0.400
0.300
0.200
0.100
0.000
350.00
400.00
500.00
600.00
700.00
nm.

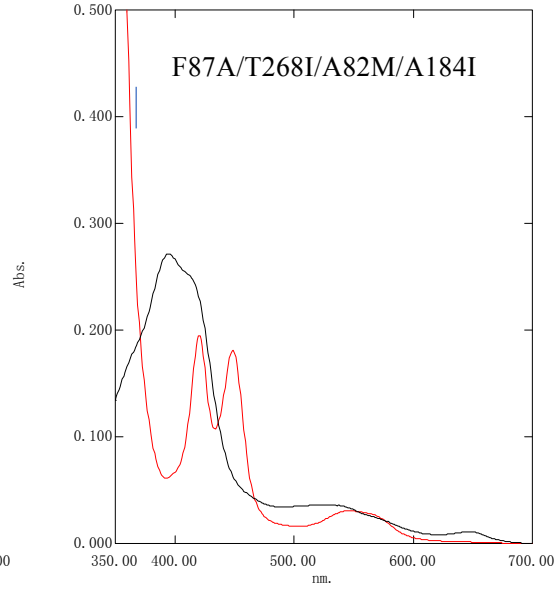
F87A/T268I/A82M/A184I
Abs.
0.500
0.400
0.300
0.200
0.100
0.000
350.00
400.00
500.00
600.00
700.00
nm.

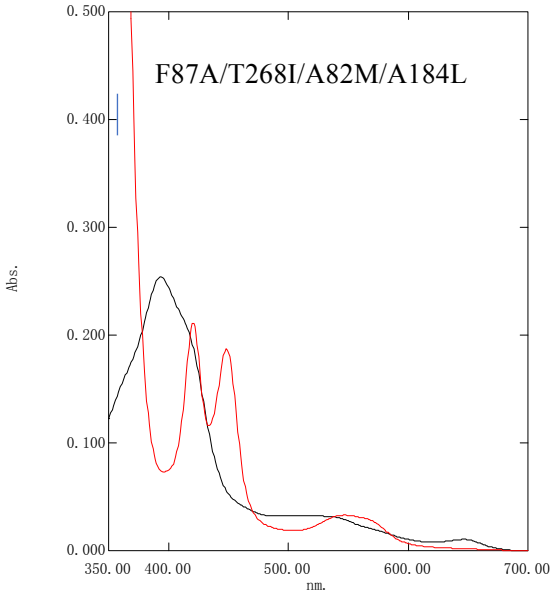
F87A/T268I/A82M/A184L
Abs.
0.500
0.400
0.300
0.200
0.100
0.000
350.00
400.00
500.00
600.00
700.00
nm.

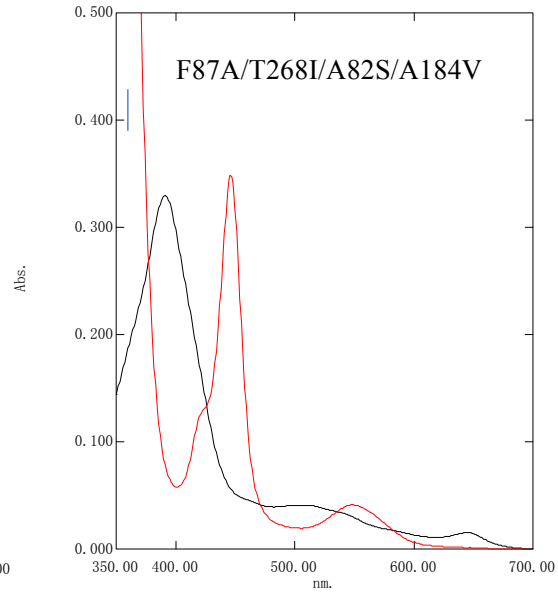
F87A/T268I/A82S/A184V
Abs.
0.500
0.400
0.300
0.200
0.100
0.000
350.00
400.00
500.00
600.00
700.00
nm.

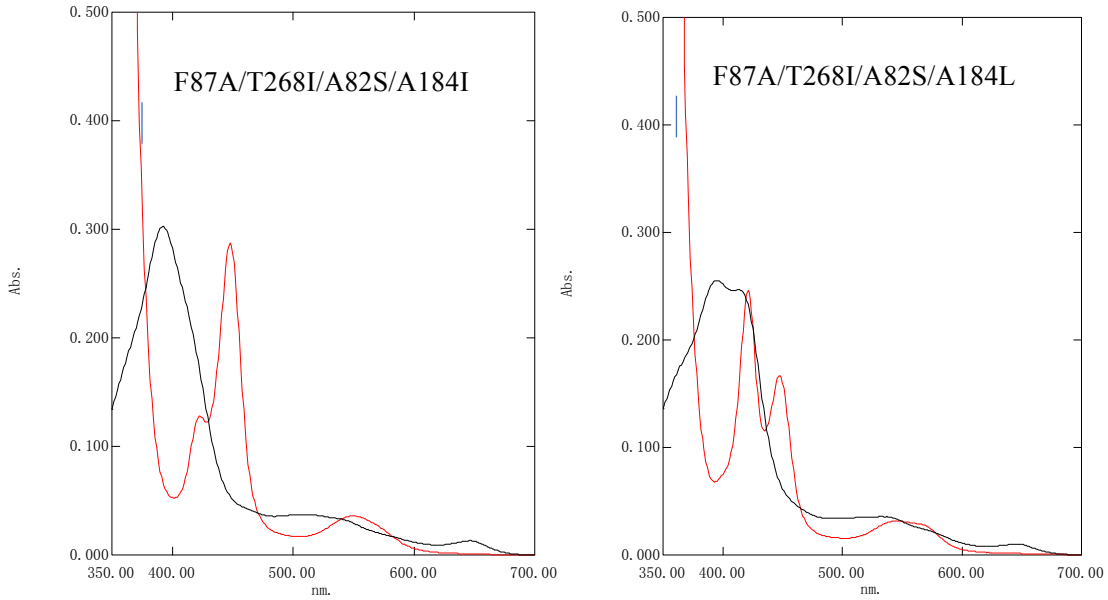

Figure S7 UV-visible spectral changes of P450BM3 mutants (black line) upon addition of $Na_2S_2O_4$ (red line) for the formation of a ferrous CO complex through the reduction of ferric heme.

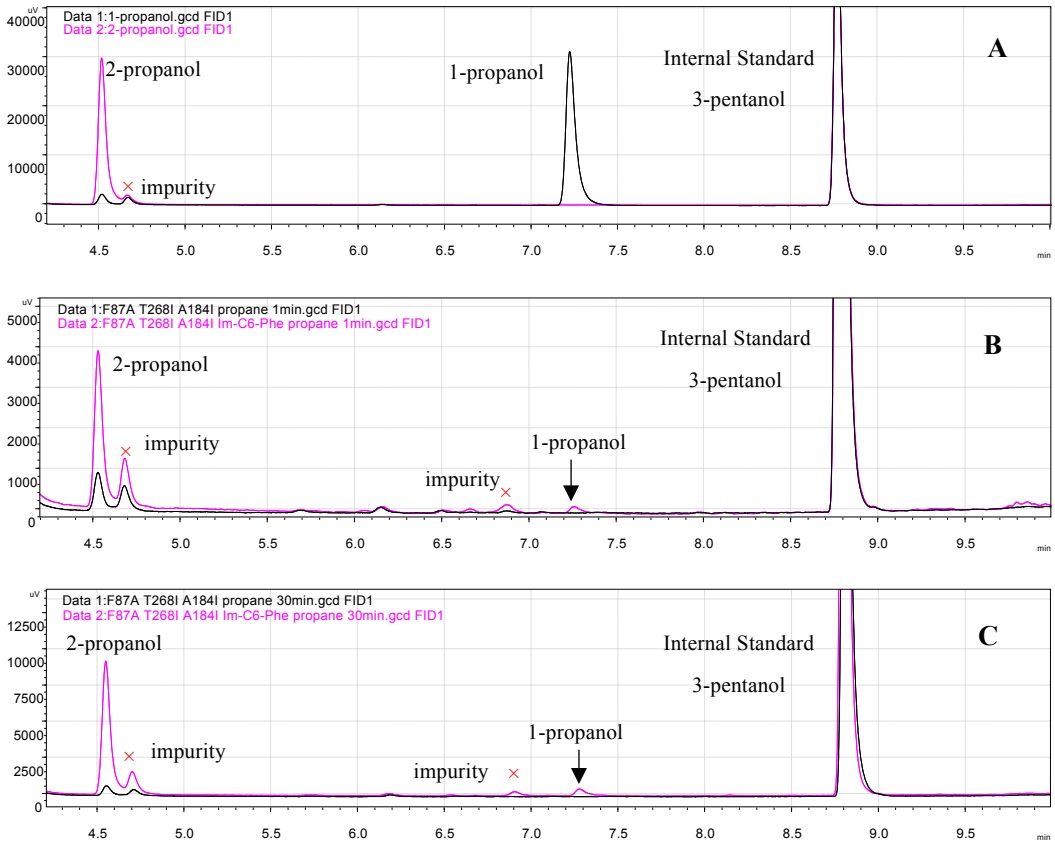

Figure S8 Typical GC analyses of the product distributions for propane hydroxylation in 60 mM H_2O_2 at 25 ℃ by F87A/T268I/A184I (0.5 μM). A) the standard samples of 1-propanol (black line) and 2-propanol (pink line); B) a 1-minute reaction results in the absence (black line) and presence (pink line) of Im-C6-Phe; C) a 30-minute reaction results in the absence (black line) and presence (pink line) of Im-C6-Phe.

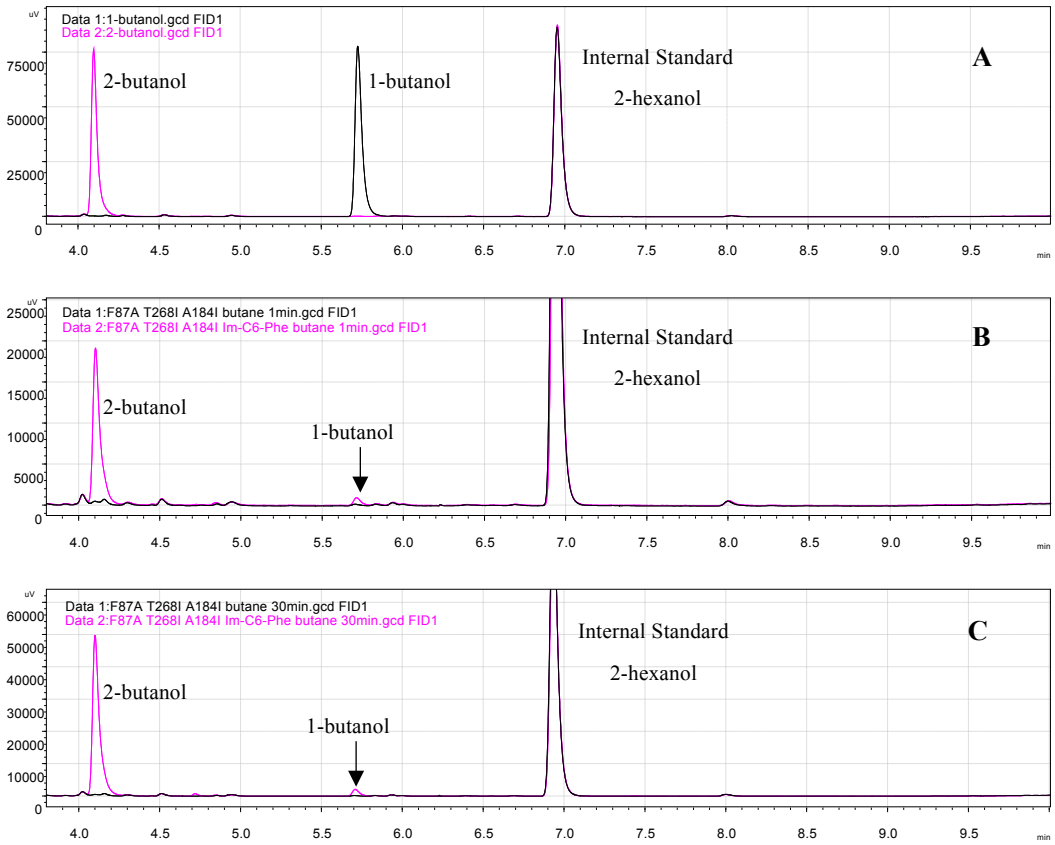

Figure S9 Typical GC analyses of the product distributions for *n*-butane hydroxylation in 60 mM H_2O_2 at 25 ℃ by F87A/T268I/A184I (0.5 μM). A) the standard samples of 1-butanol (black line) and 2-butanol (pink line); B) a 1-minute reaction results in the absence (black line) and presence (pink line) of Im-C6-Phe; C) a 30-minute reaction results in the absence (black line) and presence (pink line) of Im-C6-Phe.

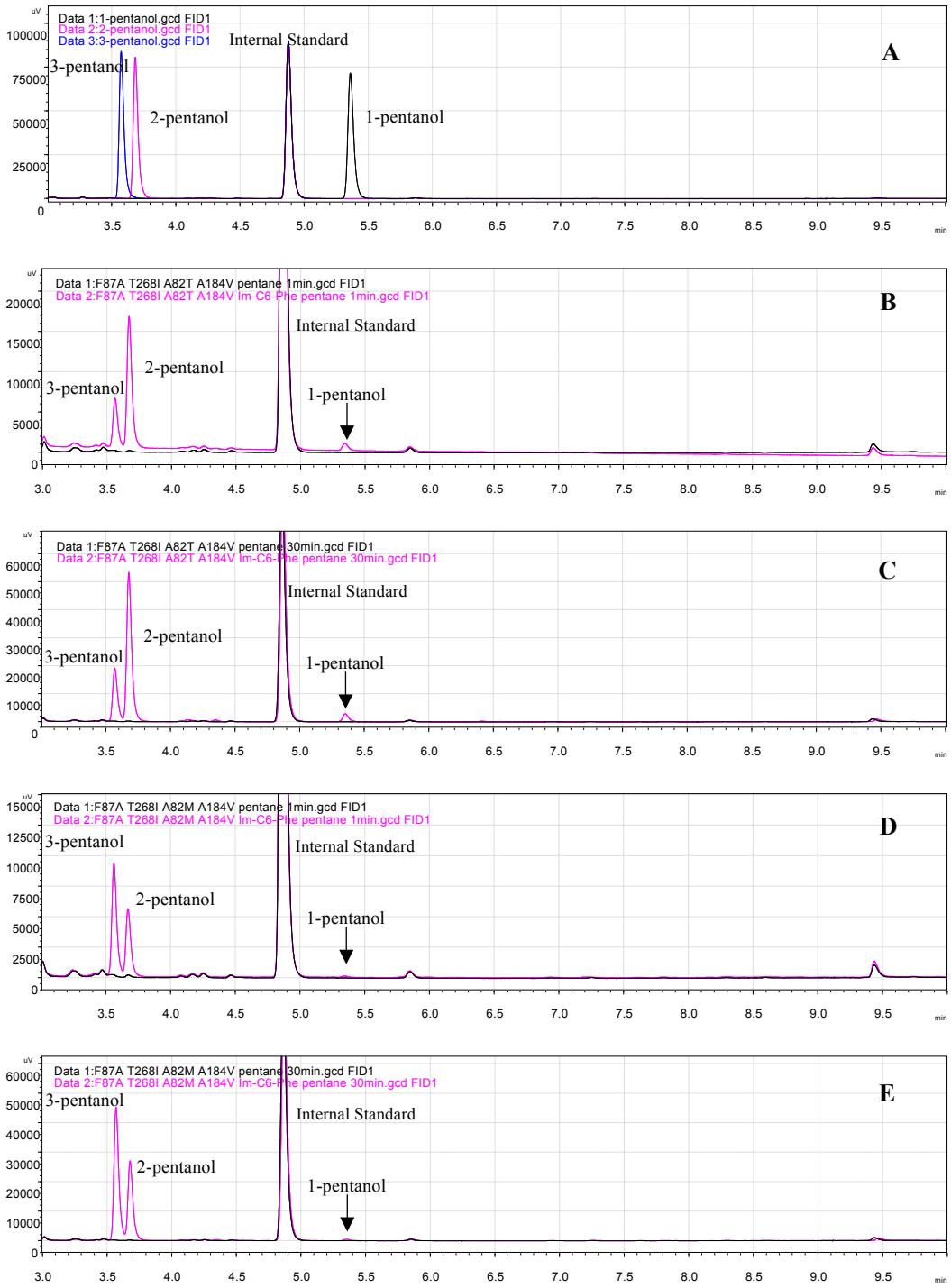

Figure S10 Typical GC analyses of the product distributions for *n*-pentane hydroxylation in 60 mM H_2O_2 at 4 ℃. A) the standard samples of 1-pentanol (black line), 2-pentanol (pink line), and 3-pentanol (blue line); B) a 1-minute reaction results by F87A/T268I/A82T/A184V (0.5 μM) in the absence (black line) and presence (pink line) of Im-C6-Phe; C) a 30-minute reaction results by F87A/T268I/A82T/A184V (0.5 μM) in the absence (black line) and presence (pink line) of Im-C6-Phe; D) a 1-minute reaction results by F87A/T268I/A82M/A184V (0.5 μM) in the absence (black line) and presence (pink line) of Im-C6-Phe; E) a 30-minute reaction results by F87A/T268I/A82M/A184V (0.5 μM) in the absence (black line) and presence (pink line) of Im-C6-Phe.

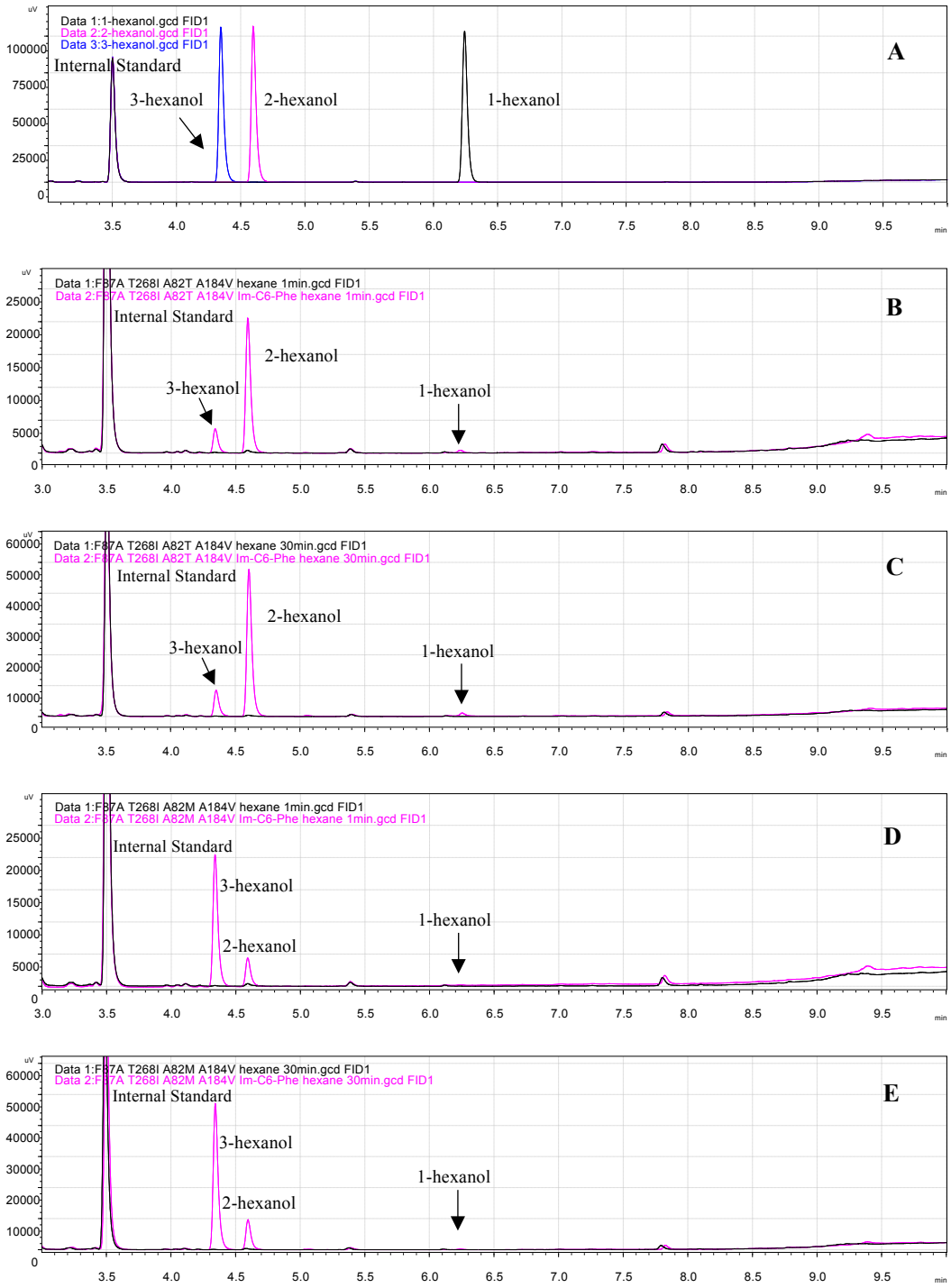

Figure S11 Typical GC analyses of the product distributions for *n*-hexane hydroxylation in 60 mM H_2O_2 at 25 ℃. A) the standard samples of 1-hexanol (black line), 2-hexanol (pink line), and 3-hexanol (blue line); B) a 1-minute reaction results by F87A/T268I/A82T/A184V (0.5 μM) in the absence (black line) and presence (pink line) of Im-C6-Phe; C) a 30-minute reaction results by F87A/T268I/A82T/A184V (0.5 μM) in the absence (black line) and presence (pink line) of Im-C6-Phe; D) a 1-minute reaction results by F87A/T268I/A82M/A184V (0.5 μM) in the absence (black line) and presence (pink line) of Im-C6-Phe; E) a 30-minute reaction results by F87A/T268I/A82M/A184V (0.5 μM) in the absence (black line) and presence (pink line) of Im-C6-Phe.

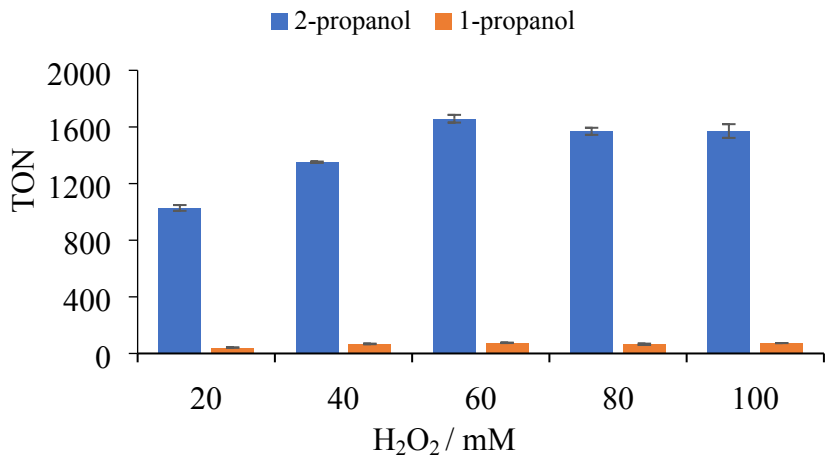

Figure S12 Optimizing the amount of H_2O_2 used in propane hydroxylation catalyzed by P450BM3 F87A/T268I/A184V mutant (0.5 μM) in the presence of Im-C6-Phe (500 μM) at 25°C.

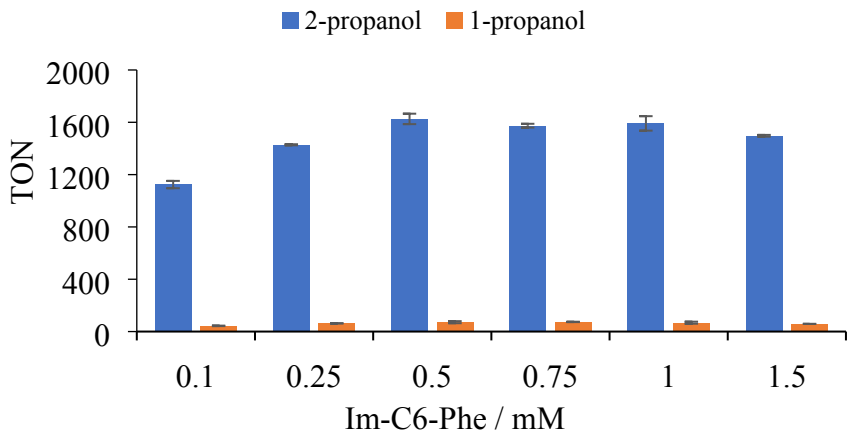

Figure S13 Optimizing the amount of Im-C6-Phe used in propane hydroxylation with H_2O_2 (60 mM) catalyzed by P450BM3 F87A/T268I/A184V mutant (0.5 μM) at 25°C.

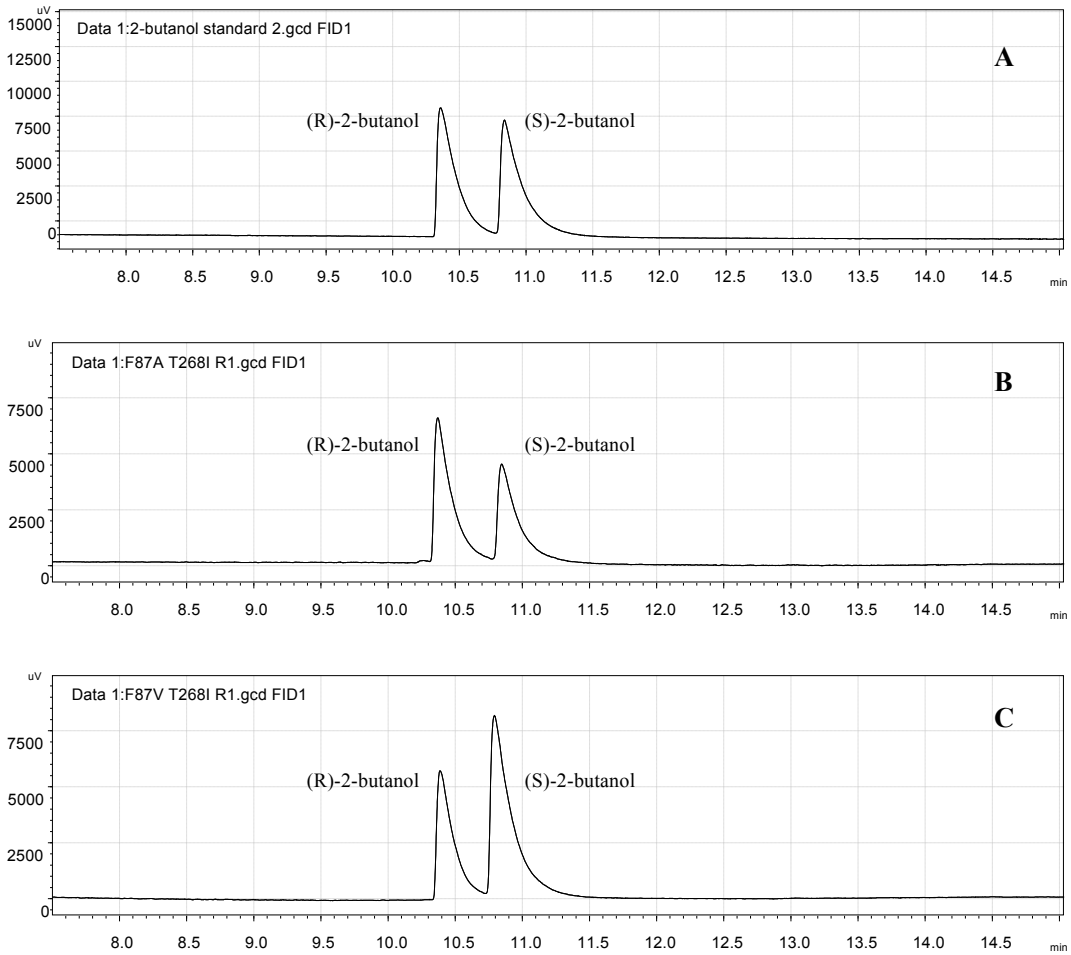

Figure S14 Typical chiral GC analyses of 2- butanol for *n*-butane hydroxylation in 60 mM H_2O_2 at 25 ℃ in the presence of Im-C6-Phe. A) the standard sample of 2-butanol; B) a 30-minute reaction results by F87A/T268I (0.5 μM); C) a 30-minute reaction results by F87V/T268I/ (0.5 μM).

Table S1 The hydroxylation of propane with H_2O_2 catalyzed by the F87 mutations of P450BM3 heme domain in the absence/presence of Im-C6-Phe[a]

mutation	TON[b]	
	No Im-C6-Phe	Im-C6-Phe
F87A	nd[c]	6±4
F87G	nd[c]	nd[c]
F87V	nd[c]	nd[c]
F87I	nd[c]	nd[c]
F87L	nd[c]	nd[c]
BMP	nd[c]	nd[c]

[a] Reaction conditions: P450BM3 (0.5 μM), H_2O_2 (20 mM), Im-C6-Phe (500 μM), in a propane-saturated pH 8.0 phosphate buffer at 25°C. [b] TON: Turnover numbers were estimated over a 30-min reaction. [c] nd: not detected.

Table S2 The hydroxylation of propane with H_2O_2 catalyzed by the double mutants of P450BM3 heme domain at the positions 87 and 268 in the presence of Im-C6-Phe[a, b]

mutation	TON[c]		
	2-propanol	1-propanol	total
F87A/T268A	9±2	nd[d]	9±2
F87A/T268V	304±5	8±1	312±6
F87A/T268I	940±7	38±1	978±8
F87A/T268L	44±1	nd[d]	44±1
F87A/T268F	nd[d]	nd[d]	nd[d]
F87A/T268W	nd[d]	nd[d]	nd[d]
F87G/T268I	35±2	nd[d]	35±2
F87V/T268I	528±10	10±2	538±12
F87I/T268I	46±1	nd[d]	46±1
F87L/T268I	46±2	nd[d]	46±2

[a] Reaction conditions: P450BM3 (0.5 μM), H_2O_2 (20 mM), Im-C6-Phe (500 μM), in a propane-saturated pH 8.0 phosphate buffer at 25°C. [b] All the control reactions did not show obvious activity of propane hydroxylation in the absence of Im-C6-Phe. [c] TON: Turnover numbers were estimated over a 30-min reaction. [d] nd: not detected.

Table S3 The hydroxylation of propane with H_2O_2 catalyzed by the triple mutants of P450BM3 heme domain at the positions 87, 268, and 82 in the presence of Im-C6-Phe[a, b]

mutation	TON[c]		
	2-propanol	1-propanol	total
F87A/T268I/A82G	237±2	8±1	245±3
F87A/T268I/A82V	351±13	13±2	364±15
F87A/T268I/A82I	307±8	13±2	320±10
F87A/T268I/A82L	396±7	17±2	413±9
F87A/T268I/A82M	374±3	16±1	390±4
F87A/T268I/A82F	nd[d]	nd[d]	nd[d]
F87A/T268I/A82S	704±9	24±1	728±10
F87A/T268I/A82T	851±15	36±1	887±16
F87A/T268I/A82C	439±2	20±1	459±3
F87A/T268I/A82D	22±4	nd[d]	22±4
F87A/T268I/A82E	62±6	nd[d]	62±6
F87A/T268I/A82N	37±2	nd[d]	37±2

[a] Reaction conditions: P450BM3 (0.5 μM), H_2O_2 (20 mM), Im-C6-Phe (500 μM), in a propane-saturated pH 8.0 phosphate buffer at 25°C. [b] All the control reactions did not show obvious activity of propane hydroxylation in the absence of Im-C6-Phe. [c] TON: Turnover numbers were estimated over a 30-min reaction. [d] nd: not detected.

Table S4 The hydroxylation of propane with H_2O_2 catalyzed by the triple mutants of P450BM3 heme domain at the positions 87, 268, and 184 in the presence of Im-C6-Phe[a, b]

mutation	TON[c]		
	2-propanol	1-propanol	total
F87A/T268I/A184V	1024±22	50±1	1074±23
F87A/T268I/A184I	1028±8	46±3	1074±11
F87A/T268I/A184L	545±3	21±1	566±4
F87A/T268I/A184M	537±7	19±2	556±9
F87A/T268I/A184F	131±10	nd[d]	131±10
F87A/T268I/A184T	907±25	37±3	944±28
F87A/T268I/A184Q	409±5	11±2	420±7
F87A/T268I/A184N	434±7	14±2	448±9

[a] Reaction conditions: P450BM3 (0.5 μM), H_2O_2 (20 mM), Im-C6-Phe (500 μM), in a propane-saturated pH 8.0 phosphate buffer at 25°C. [b] All the control reactions did not show obvious activity of propane hydroxylation in the absence of Im-C6-Phe. [c] TON: Turnover numbers were estimated over a 30-min reaction. [d] nd: not detected.

Table S5 The hydroxylation of propane with H_2O_2 catalyzed by the quadruple mutants of P450BM3 heme domain at the positions 87, 268, 82, and 184 in the presence of Im-C6-Phe[a, b]

mutation	TON[c]		
	2-propanol	1-propanol	total
F87A/T268I/A82T/A184V	891±15	40±1	931±16
F87A/T268I/A82T/A184I	846±24	38±1	884±25
F87A/T268I/A82T/A184L	566±16	23±1	589±17
F87A/T268I/A82V/A184V	623±26	30±3	653±29
F87A/T268I/A82V/A184I	622±4	28±1	650±5
F87A/T268I/A82V/A184L	273±3	12±1	285±4
F87A/T268I/A82S/A184V	842±8	35±2	877±10
F87A/T268I/A82S/A184I	850±7	32±1	882±8
F87A/T268I/A82S/A184L	363±12	13±1	376±13
F87A/T268I/A82M/A184V	494±5	20±1	514±6
F87A/T268I/A82M/A184I	320±9	11±1	331±10
F87A/T268I/A82M/A184L	189±11	7±1	196±12

[a] Reaction conditions: P450BM3 (0.5 μM), H_2O_2 (20 mM), Im-C6-Phe (500 μM), in a propane-saturated pH 8.0 phosphate buffer at 25°C. [b] All the control reactions did not show obvious activity of propane hydroxylation in the absence of Im-C6-Phe. [c] TON: Turnover numbers were estimated over a 30-min reaction.

Table S6 The hydroxylation of *n*-butane with H_2O_2 catalyzed by the triple mutants of P450BM3 heme domain at the positions 87, 268, and 82 in the presence of Im-C6-Phe[a, b]

mutation	TON[c]		
	2-butanol	1-butanol	total
F87A/T268I/A82G	408±11	25±4	433±15
F87A/T268I/A82V	992±15	40±1	1032±16
F87A/T268I/A82I	790±9	40±1	830±10
F87A/T268I/A82L	1185±25	57±1	1242±26
F87A/T268I/A82M	425±3	20±1	445±4
F87A/T268I/A82F	48±1	7±1	55±2
F87A/T268I/A82S	1093±60	47±3	1140±63
F87A/T268I/A82T	1467±8	60±1	1527±9
F87A/T268I/A82C	772±20	40±2	812±22
F87A/T268I/A82D	nd[d]	nd[d]	nd[d]
F87A/T268I/A82E	83±2	nd[d]	83±2
F87A/T268I/A82N	72±1	nd[d]	72±1

[a] Reaction conditions: P450BM3 (0.5 μM), H_2O_2 (20 mM), Im-C6-Phe (500 μM), in a butane-saturated pH 8.0 phosphate buffer at 25°C. [b] All the control reactions did not show obvious activity of *n*-butane hydroxylation in the absence of Im-C6-Phe. [c] TON: Turnover numbers were estimated over a 30-min reaction. [d] nd: not detected.

Table S7 The hydroxylation of *n*-butane with H_2O_2 catalyzed by the triple-mutation of P450BM3 heme domain at the positions 87, 268, and 184 in the presence of Im-C6-Phe[a, b]

mutation	TON[c]		
	2-butanol	1-butanol	total
F87A/T268I/A184V	1851±21	76±2	1927±23
F87A/T268I/A184I	1986±19	72±1	2057±20
F87A/T268I/A184L	1360±9	50±1	1410±10
F87A/T268I/A184M	1009±15	38±1	1047±16
F87A/T268I/A184F	356±5	18±1	374±6
F87A/T268I/A184T	1421±1	58±1	1479±2
F87A/T268I/A184Q	960±1	37±1	997±2
F87A/T268I/A184N	783±10	31±1	814±11

[a] Reaction conditions: P450BM3 (0.5 μM), H_2O_2 (20 mM), Im-C6-Phe (500 μM), in a butane-saturated pH 8.0 phosphate buffer at 25°C. [b] All the control reactions did not show obvious activity of *n*-butane hydroxylation in the absence of Im-C6-Phe. [c] TON: Turnover numbers were estimated over a 30-min reaction.

Table S8 The PFRs of *n*-butane hydroxylation with H_2O_2 catalyzed by P450BM3 mutants in the presence of Im-C6-Phe[a, b]

mutation	PFR[c]		
	2-butanol	1-butanol	total
F87V/T268I	913±14	18±1	931±15
F87A/T268I	902±32	37±1	939±33
F87A/T268I/A82T	1042±6	43±1	1085±7
F87A/T268I/A82S	832±21	32±1	864±22
F87A/T268I/A184V	992±12	41±1	1033±13
F87A/T268I/A184I	979±9	37±1	1016±10
F87A/T268I/A82T/A184I	932±6	36±1	968±7
F87A/T268I/A82S/A184I	816±23	31±1	847±24

[a] Reaction conditions: P450BM3 (0.5 μM), H_2O_2 (60 mM), Im-C6-Phe (500 μM), in a butane-saturated pH 8.0 phosphate buffer at 25°C. [b] All the control reactions did not show obvious activity of *n*-butane hydroxylation in the absence of Im-C6-Phe. [c] PFR: Product formation rates were estimated as $\mu mol \cdot min^{-1} \cdot (\mu mol\ P450)^{-1}$ over a 1-min reaction.

Table S9 The TONs of *n*-butane hydroxylation with H_2O_2 catalyzed by P450BM3 mutants in the presence of Im-C6-Phe[a, b]

mutation	TON[c]			Ratio[d]
	2-butanol	1-butanol	total	
F87V/T268I	2009±11	29±1	2038±12	99:1
F87A/T268I	1882±6	67±1	1949±7	97:3
F87A/T268I/A82T	2253±20	87±1	2340±21	96:4
F87A/T268I/A82S	1830±58	63±3	1893±61	97:3
F87A/T268I/A184V	2262±1	87±1	2349±2	96:4
F87AT268I/A184I	2289±18	79±1	2368±19	97:3
F87A/T268I/A82T/A184I	2088±23	74±1	2162±24	97:3
F87A/T268I/A82S/A184I	1759±15	59±1	1818±16	97:3

[a] Reaction conditions: P450BM3 (0.5 μM), H_2O_2 (60 mM), Im-C6-Phe (500 μM), in a butane-saturated pH 8.0 phosphate buffer at 25°C. [b] All the control reactions did not show obvious activity of *n*-butane hydroxylation in the absence of Im-C6-Phe. [c] TON: Turnover numbers were estimated over a 30-min reaction. [d] Ratio: 2-butanol/1-butanol.

Table S10 The enantiomeric excess of 2-butanol (ee%) for *n*-butane hydroxylation with H_2O_2 catalyzed by P450BM3 mutants in the presence of Im-C6-Phe[a]

mutations	2-butanol / ee%
F87V/T268I	28 (S)
F87A/T268I	14 (R)
F87A/T268I/A82T	13 (R)
F87A/T268I/A82S	14 (R)
F87A/T268I/A184V	10 (R)
F87AT268I/A184I	11 (R)
F87A/T268I/A82T/A184I	11 (R)
F87A/T268I/A82S/A184I	11 (R)

[a] Reaction conditions: P450BM3 (0.5 μM), H_2O_2 (60 mM), Im-C6-Phe (500 μM), in a butane-saturated pH 8.0 phosphate buffer at 25°C.

Table S11 The TONs of *n*-pentane hydroxylation with H_2O_2 catalyzed by P450BM3 mutants in the presence of Im-C6-Phe[a, b]

mutation	TON[c]				Ratio[d]
	3-pentanol	2-pentanol	1-pentanol	total	
F87V/T268I	226±2	860±5	6±1	1092±8	21:79: <0.5
F87A/T268I	345±8	654±14	57±1	1056±23	33:62:5
F87A/T268I/A82T	331±9	943±27	67±2	1341±38	25:70:5
F87A/T268I/A82M	751±8	403±4	10±1	1164±13	64:35:1
F87A/T268I/A184V	384±1	869±1	66±1	1319±3	29:66:5
F87A/T268I/A184I	478±9	917±17	68±1	1463±27	33:63:4
F87A/T268I/A82T/A184V	391±8	1174±23	75±2	1640±33	24:72:4
F87A/T268I/A82M/A184V	930±8	611±6	12±1	1553±15	60:39:1

[a] Reaction conditions: P450BM3 (0.5 μM), *n*-pentane (6 mM), H_2O_2 (60 mM), Im-C6-Phe (500 μM), in pH 8.0 phosphate buffer at 4°C. [b] All the control reactions did not show obvious activity of *n*-pentane hydroxylation in the absence of Im-C6-Phe. [c] TON: Turnover numbers were estimated over a 30-min reaction. [d] Ratio: 3-pentanol/2-pentanol/1-pentanol.

Table S12 The TONs of *n*-hexane hydroxylation with H_2O_2 catalyzed by P450BM3 mutants in presence of Im-C6-Phe[a, b]

mutation	TON[c]				Ratio[d]
	3-hexanol	2-hexanol	1-hexanol	total	
F87V/T268I	65±2	301±3	4±1	370±6	17:82:1
F87A/T268I	88±3	669±2	18±1	775±6	12:86:2
F87A/T268I/A82T	141±1	843±3	19±1	1003±5	14:84:2
F87A/T268I/A82M	719±1	146±1	3±1	868±3	82:18:<0.3
F87A/T268I/A184V	140±1	1038±3	25±1	1203±5	12:86:2
F87A/T268I/A184I	176±2	1085±1	25±1	1286±4	14:84:2
F87A/T268I/A82T/A184V	193±1	1107±2	22±1	1322±4	15:84:1
F87A/T268I/A82M/A184V	1095±18	234±3	4±1	1333±22	81:19:<0.3

[a] Reaction conditions: P450BM3 (0.5 μM), *n*-hexane (6 mM), H_2O_2 (60 mM), Im-C6-Phe (500 μM), in pH 8.0 phosphate buffer at 25°C. [b] All the control reactions did not show obvious activity of *n*-hexane hydroxylation in the absence of Im-C6-Phe. [c] TON: Turnover numbers were estimated over a 30-min reaction. [d] Ratio: 3-hexanol/2-hexanol/1-hexanol.

Table S13 The hydroxylation of *n*-pentane with H_2O_2 catalyzed by the triple mutants of P450BM3 heme domain at the positions 87, 268, and 184 in the presence of Im-C6-Phe[a, b]

mutation	TON[c]				Ratio[d]
	3-pentanol	2-pentanol	1-pentanol	total	
F87A/T268I/A184V	288±6	638±14	49±1	975±21	30:65:5
F87A/T268I/A184I	324±12	605±21	45±2	974±35	33:62:5
F87A/T268I/A184L	216±13	426±25	30±2	672±40	32:63:5
F87A/T268I/A184M	214±2	361±2	28±1	603±5	35:60:5
F87A/T268I/A184F	52±2	101±5	7±1	160±8	33:63:4
F87A/T268I/A184T	208±1	430±1	35±1	673±3	31:64:5
F87A/T268I/A184Q	185±10	308±16	24±2	517±28	35:60:5
F87A/T268I/A184N	157±9	278±14	21±2	456±25	34:61:5

[a] Reaction conditions: P450BM3 (0.5 μM), *n*-pentane (4 mM), H_2O_2 (20 mM), Im-C6-Phe (500 μM), in pH 8.0 phosphate buffer at 4°C. [b] All the control reactions did not show obvious activity of *n*-pentane hydroxylation in the absence of Im-C6-Phe. [c] TON: Turnover numbers were estimated over a 30-min reaction. [d] Ratio: 3-pentanol/2-pentanol/1-pentanol.

Table S14 The hydroxylation of *n*-hexane with H_2O_2 catalyzed by the triple mutants of P450BM3 heme domain at the positions 87, 268, and 184 in the presence of Im-C6-Phe[a, b]

mutation	TON[c]				Ratio[d]
	3-hexanol	2-hexanol	1-hexanol	total	
F87A/T268I/A184V	112±4	854±21	20±2	986±27	11:87:2
F87A/T268I/A184I	124±3	808±3	17±1	949±7	13:85:2
F87A/T268I/A184L	68±1	331±1	6±1	405±3	17:82:1
F87A/T268I/A184M	68±2	472±3	11±2	551±7	12:86:2
F87A/T268I/A184F	10±2	58±5	nd[e]	68±7	15:85:0
F87A/T268I/A184T	79±6	614±2	15±1	708±9	11:87:2
F87A/T268I/A184Q	52±7	282±2	5±1	339±10	16:83:1
F87A/T268I/A184N	44±3	228±9	nd[c]	272±12	16:84:0

[a] Reaction conditions: P450BM3 (0.5 μM), *n*-hexane (4 mM), H_2O_2 (20 mM), Im-C6-Phe (500 μM), in pH 8.0 phosphate buffer at 25°C. [b] All the control reactions did not show obvious activity of *n*-hexane hydroxylation in the absence of Im-C6-Phe. [c] TON: Turnover numbers were estimated over a 30-min reaction. [d] Ratio: 3-hexanol/2-hexanol/1-hexanol. [e] nd: not detected.

Table S15 The hydroxylation of *n*-pentane with H_2O_2 catalyzed by the triple mutants of P450BM3 heme domain at the positions 87, 268, and 82 in the presence of Im-C6-Phe[a, b]

mutation	TON[c]				Ratio[d]
	3-pentanol	2-pentanol	1-pentanol	total	
F87A/T268I/A82G	115±3	190±5	15±1	320±9	36:59:5
F87A/T268I/A82V	163±3	375±9	30±1	568±13	29:66:5
F87A/T268I/A82I	121±5	331±15	16±1	468±21	26:71:3
F87A/T268I/A82L	149±5	467±18	21±1	637±24	23:74:3
F87A/T268I/A82M	380±1	203±1	4±1	587±6	65:34:1
F87A/T268I/A82F	nd[e]	nd[e]	nd[e]	nd[e]	-
F87A/T268I/A82S	223±7	416±13	37±2	676±22	33:62:5
F87A/T268I/A82T	252±1	711±3	54±1	1017±5	25:70:5
F87A/T268I/A82C	156±1	484±1	37±1	677±3	23:72:5
F87A/T268I/A82D	nd[e]	nd[e]	nd[e]	nd[e]	-
F87A/T268I/A82E	14±1	25±1	nd[e]	39±2	36:64:0
F87A/T268I/A82N	13±1	25±1	nd[e]	38±2	34:66:0

[a] Reaction conditions: P450BM3 (0.5 μM), *n*-pentane (4 mM), H_2O_2 (20 mM), Im-C6-Phe (500 μM), in pH 8.0 phosphate buffer at 4°C. [b] All the control reactions did not show obvious activity of *n*-pentane hydroxylation in the absence of Im-C6-Phe. [c] TON: Turnover numbers were estimated over a 30-min reaction. [d] Ratio: 3-pentanol/2-pentanol/1-pentanol. [e] nd: not detected.

Table S16 The hydroxylation of *n*-hexane with H_2O_2 catalyzed by the triple mutants of P450BM3 heme domain at the positions 87, 268, and 82 in the presence of Im-C6-Phe[a, b]

mutation	TON[c]				Ratio[d]
	3-hexanol	2-hexanol	1-hexanol	total	
F87A/T268I/A82G	17±1	96±4	nd[e]	113±5	15:85:0
F87A/T268I/A82V	43±2	455±24	11±1	509±27	9:89:2
F87A/T268I/A82I	146±3	235±5	4±1	385±9	38:61:1
F87A/T268I/A82L	291±10	396±13	7±1	694±24	42:57:1
F87A/T268I/A82M	404±2	87±1	2±1	492±4	82:18: <0.3
F87A/T268I/A82F	nd[e]	nd[e]	nd[e]	nd[e]	-
F87A/T268I/A82S	42±1	411±7	14±2	467±10	9:88:3
F87A/T268I/A82T	113±3	772±31	18±1	903±35	12:86:2
F87A/T268I/A82C	62±1	331±4	7±1	400±6	15:83:2
F87A/T268I/A82D	nd[e]	nd[e]	nd[e]	nd[e]	-
F87A/T268I/A82E	nd[e]	nd[e]	nd[e]	nd[e]	-
F87A/T268I/A82N	nd[e]	nd[e]	nd[e]	nd[e]	-

[a] Reaction conditions: P450BM3 (0.5 μM), *n*-hexane (4 mM), H_2O_2 (20 mM), Im-C6-Phe (500 μM), in pH 8.0 phosphate buffer at 25°C. [b] All the control reactions did not show obvious activity of *n*-hexane hydroxylation in the absence of Im-C6-Phe. [c] TON: Turnover numbers were estimated over a 30-min reaction. [d] Ratio: 3-hexanol/2-hexanol/1-hexanol. [e] nd: not detected.

Table S17 The PFRs of *n*-pentane hydroxylation with H_2O_2 catalyzed by P450BM3 mutants in the presence of Im-C6-Phe[a, b]

mutation	PFR[c]			
	3-pentanol	2-pentanol	1-pentanol	total
F87V/T268I	48±1	184±5	1±0	233±6
F87A/T268I	109±3	192±5	17±1	318±9
F87A/T268I/A82T	116±1	304±4	22±1	442±6
F87A/T268I/A82M	186±8	99±4	2±1	187±13
F87A/T268I/A184V	119±3	250±6	20±1	391±10
F87A/T268I/A184I	131±5	234±10	18±1	383±16
F87A/T268I/A82T/A184V	127±4	364±11	25±1	516±16
F87A/T268I/A82M/A184V	196±3	129±1	3±1	328±5

[a] Reaction conditions: P450BM3 (0.5 μM), pentane (6 mM), H_2O_2 (60 mM), Im-C6-Phe (500 μM), in pH 8.0 phosphate buffer at 4°C. [b] All the control reactions did not show obvious activity of *n*-pentane hydroxylation in the absence of Im-C6-Phe. [c] PFR: Product formation rates were estimated as $\mu mol \cdot min^{-1} \cdot (\mu mol\ P450)^{-1}$ over a 1-min reaction.

Table S18 The PFRs of *n*-hexane hydroxylation with H_2O_2 catalyzed by P450BM3 mutants in presence of Im-C6-Phe[a, b]

mutation	PFR[c]			
	3-hexanol	2-hexanol	1-hexanol	total
F87V/T268I	30±2	139±7	2±1	171±10
F87A/T268I	34±1	251±12	6±1	291±14
F87A/T268I/A82T	65±1	390±5	9±1	464±7
F87A/T268I/A82M	332±9	74±2	1±0	407±11
F87A/T268I/A184V	53±1	388±2	9±1	450±4
F87A/T268I/A184I	61±1	370±2	8±1	439±4
F87A/T268I/A82T/A184V	88±1	502±9	10±1	600±11
F87A/T268I/A82M/A184V	449±15	103±4	2±1	554±20

[a] Reaction conditions: P450BM3 (0.5 μM), hexane (6 mM), H_2O_2 (60 mM), Im-C6-Phe (500 μM), in pH 8.0 phosphate buffer at 25°C. [b] All the control reactions did not show obvious activity of *n*-hexane hydroxylation in the absence of Im-C6-Phe. [c] PFR: Product formation rates were estimated as $\mu mol \cdot min^{-1} \cdot (\mu mol\ P450)^{-1}$ over a 1-min reaction.

References

[1] Ma, N.; Chen, Z.; Chen, J.; Chen, J.; Wang, C.; Zhou, H.; Yao, L.; Shoji, O.; Watanabe, Y.; Cong, Z. Dual-functional small molecules for generating an efficient cytochrome P450BM3 peroxygenase. *Angew. Chem. Int. Ed.* **2018**, *57*, 7628-7633.

[2] Omura, T.; Sato, R. The carbon monoxide-binding pigment of liver microsomes. I. evidence for its hemoprotein nature. *J. Biol. Chem.* **1964**, *239*, 2370-2378.

[3] Wang, Z. J.; Renata, H.; Peck, N. E.; Farwell, C. C.; Coelho, P. S.; Arnold, F. H. Improved cyclopropanation activity of histidine-ligated cytochrome P450 enables the enantioselective formal synthesis of levomilnacipran. *Angew. Chem. Int. Ed.* **2014**, *53*, 6810-6813.